OWTNM 2023

XXIX International Workshop on Optical Wave & Waveguide Theory and Numerical Modelling

Marseille, France, 4 & 5 May 2023

Local organizing committee from the Institut Fresnel

INSTITUT FRESNEL MARSEILLE

Aix*Marseille université Socialement engagée

cnrs

Centrale Méditerranée

Acknowledgments

The organizers thank for their interest and support:

- Aix-Marseille Université (AMU) which provides the amphitheatre, the poster room, and staff members on its Saint-Charles campus
- The Institut Archimède of AMU for its funding
- The Institut AMUtech of AMU for its funding
- The ECM, Ecole Centrale Méditerranée, for its funding
- The Institut Fresnel, our laboratory, for its funding
- The CNRS region administration for the management of the inscriptions by its online tool "Azur Colloque"
- The communication officer and the two implied financial managers of the Institut Fresnel for their useful and efficient help
- The OWTNM scientific committee members for the invited speakers suggestions
- Mandfred Hammer of the University of Paderborn for his unfailing support

Institut
Matériaux Avancés
et Nanotechnologies
Aix*Marseille Université

Institut
Archimède
Mathématiques-Informatique
Aix*Marseille Université

Preface

The XXIX International Workshop on Optical Wave $_{\&\,\mathrm{Waveguide}}$ Theory and Numerical Modelling (OWTNM 2023) is scheduled on May, 4-5, 2023 in Marseille (France), at the Saint-Charles campus. The previous OWTNM edition hold in Berlin (Germany) in February 2020, and was collocated with the 14^{th} Annual Meeting Photonic Devices of Zuse Institute. The combined workshop was entitled Theoretical and Numerical Tools for Nanophotonics (TNTN 2020).
After three years of absence due to the Covid 19 pandemic, including an unfortunately canceled TNTN 2021 in Bordeaux (France), we look forward to seeing in Marseille the regular attendees of the workshop, together with participants who will come to OWTNM for the first time. We hope and expect that this edition of OWTNM will be as successful as the previous meetings. The workshop will host seven oral sessions ensuring thirty-two talks, and the usual poster session.

The website of OWTNM 2023 is available at the following link:
`https://www.fresnel.fr/spip/spip.php?article2764`

The website of the OWTNM workshop series is available at the following link:
`https://www.owtnm.eu/`

Marseille, 20^{th} April 2023.
For the local organizing committee of OWTNM 2023:
Anne-Laure FEHREMBACH, and Gilles RENVERSEZ (Institut Fresnel, Marseille, France).

Contents

Programme

Workshop schedule

Full poster list

OWTNM 2023 – Detailed schedule

Venue : Marseille St-Charles Campus (3 place Victor Hugo, 13331 Marseille Cedex 3)
Amphitheatre « Sciences naturelles »

Begin	End	Dura-tion	Thursday, May 4
08:20	08:50	00:30	*Welcoming (badge distribution)*
08:50	09:00	00:10	*Opening of the workshop : Anne-Laure Fehrembach, Gilles Renversez (Institut Fresnel, France)*
			1 – Theory and modelling 1 (9h-10h50)
09:00	09:35	00:35	Nahid TALEBI (invited): Electron-light Interactions Simulated with Multiscale Maxwell-Schrödinger Framework
09:35	09:53	00:18	Guillaume DEMESY : Open source finite element models for photonics with ONELAB/Gmsh/GetDP
09:53	10:11	00:18	Paula NUNO-RUANO : Modelling and engineering of the optomechanical coupling in subwavelength-structured silicon waveguides
10:11	10:29	00:18	Tong WU : MAN: A freeware to compute and analyze modes of resonators
10:29	10:47	00:18	Mandana JALALI : Coated Microtoroid versus Coated Microsphere for Biosensing Applications
10:50	11:20	00:30	*Coffee break*
			2 – Machine learning (11h20-12h35)
11:20	11:38	00:18	Sendy PHANG : Numerical Demonstration of a Photonic Reservoir Computing Based on a Stimulated Brillouin Scattering System
11:38	11:56	00:18	Gleb ANUFRIEV : Time-Delayed Photonic Reservoir Computing for Chemical Sensing
11:56	12:14	00:18	Andrei V. ERMOLAEV : Identifying extreme localization and rogue waves in fibre optics modulation instability using data-driven dominant balance
12:14	12:32	00:18	Mehdi MABED : Machine Learning analysis of Continuous Wave fiber Modulation Instability
12:35	14:00	01:25	*Lunch break*
			3 – Theory and modelling 2 (14h-15h30)
14:00	14:35	00:35	Ana VUKOVIC (invited): Recent advances in Modelling Photonic Crystal Surface Emitting Lasers (PCSELs) Using Unstructured Transmission Line (UTLM) Modelling Method
14:35	14:53	00:18	Herve TORTEL : FETI method applied to the scattering studies of long resonant structures
14:53	15:11	00:18	Anurag SHARMA : Full Vectorial 3-D Non-Paraxial Beam Propagation Method
15:11	15:29	00:18	Chun-Fang LI : No circular birefringence exists in a chiral medium
15:30	16:00	00:30	*Coffee break*
			4 – Integrated optics 1 (16h-17h50)
16:00	16:35	00:35	José-Manuel LUQUE-GONZALES (invited, on behalf of Pavel CHEBEN) : Anisotropy engineered metamaterials for polarization and mode management in integrated photonics
16:35	16:53	00:18	Nikos FAYARD : The comb waveguide: a new tool for Waveguide QED
16:53	17:11	00:18	Maria PASZKIEWICZ : Approximation methods for the fast calculation of transmission of photonic wire bonds
17:11	17:29	00:18	Anurag SHARMA : A Propagation Method for Higher Order Modes in Fiber Structures
17:29	17:47	00:18	Ajay KUMAR : Beam Propagation Analysis for Bragg Fibers
19:30	23:30	04:00	*Conference dinner : restaurant La Nautique (pavillon flottant, Quai de rive neuve, 13007 MARSEILLE)*

Begin	End	Dura-tion	Friday, May 5
08:20	08:40	00:20	*Welcoming (badge distribution)*
			5 – Integrated optics 2 (8h40-10h30)
08:40	09:15	00:35	Delphine MARRIS-MORINI (invited): SiGe photonics circuits for the mid-IR wavelength range
09:15	09:33	00:18	Jonathan PELTIER : DC Kerr effect for high speed modulation
09:33	09:51	00:18	Enakshi K. SHARMA : Design Strategy for Compact Mode-Division-Multiplexer for Multi-Channel Optical Interconnects
09:51	10:09	00:18	Manfred HAMMER : Lossless operation of high-contrast integrated optical waveguide gratings
10:09	10:27	00:18	Gilles RENVERSEZ : Modelling of a fully integrated graphene-based compact plasmon coupler
10:30	11:00	00:30	*Coffee break*
			Posters (11h-12h30) – Espace Pouillon
12:30	14:00	01:30	*Lunch break*
			6 – Inverse design (14h-15h30)
14:00	14:35	00:35	Benjamin VIAL (invited): Optimizing photonic devices: open-source implementation of auto-differentiable numerical methods
14:35	14:53	00:18	Enzo ISNARD : Advancing wavefront shaping with resonant metasurface
14:53	15:11	00:18	Søren Engelberth HANSEN : Inverse design of compact and broadband nanophotonic beam-splitters
15:11	15:29	00:18	Antoine MOREAU : Physically understandable photonic structures generated by optimization
15:30	16:00	00:30	*Coffee break*
			7 – Theory and modelling 3 (16h-17h30)
16:00	16:18	00:18	Nicolas LEBBE : Homogenization and optimization of plasmonic metasurfaces
16:18	16:36	00:18	Emmanuel ROUSSEAU : On the Generalized Snell-Descartes laws for metasurfaces
16:36	16:54	00:18	Ya Yan LU : A General Theory on the Robustness of Bound States in the Continuum
16:54	17:12	00:18	Brian STOUT : Leaky modes for waveguide response functions
17:12	17:30	00:18	Isam BEN SOLTANE : A description of MOSEM (Multiple-Order Singularity Expansion Method) and its interest for studying light scattering
17:30	17:40	00:10	*Closing of the workshop*

List of posters

P1 *Modelling of light scattering in resonant multilayered stacks*
Toumi Yousra, Lereu Aude, Demésy Guillaume, Lumeau Julien, Favard Cyril, Lemarchand Fabien

P2 *3D simulation of broad rejection band and ultra-narrow bandwidth hybrid Fabry-Pérot for guided optics*
Bittebierre Jean

P3 *Map of transmission coefficients for open bent waveguides with constant curvature*
Sukhova Mariia, Paszkiewicz Maria, Dörfler Willy, Rockstuhl Carsten

P4 *Comparison of boundary integral equation methods for photonic crystal fibers with Comsol Multiphysics simulation*
Ayela Marc-Amour

P5 *Vector Mode Propagation in Graded Index Ring Core Fibers*
Choudhary Pratiksha, Sharma Anurag

P6 *Design of nanostructured blazed gratings for spectro-imagers in space*
Ans Simon, Demésy Guillaume, Zamkotsian Frédéric

P7 *Reliable automated classification of symmetry-induced degeneracy for numerically calculated guided modes*
Lüder Hannes, Uvarov Alexander, Mingaleev Sergei, Koltchanov Igor, Richter André

P8 *Second harmonic generation in cavity-resonator integrated grating couplers*
Fehrembach Anne-Laure, Popov Evgeny, Tortel Hervé, Hemsley Elisabeth, Monmayrant Antoine, Gauthier-Lafaye Olivier, Calvez Stéphane

Oral presentations

Electron-light Interactions Simulated with Multiscale Maxwell-Schrödinger Framework

N. Talebi[1,*]
[1]Institute for Experimental and Applied Physics, Kiel University, Leibnizstr. 19, 24118 Kiel, Germany

*talebi@physik.uni-kiel.de

The interaction between free electron wavepackets and optical near-fields are intensively researched for devising ultrafast and quantum-sensitive measurement schemes. Here, the dynamics of electron wavepackets evolving in the near-field zone of nanostructures are simulated using a Maxwell-Schrödinger toolbox.

Introduction

Nowadays, investigating the dynamics of materials excitations with electron microscopes have been made possible, by combing light and electron sources in a unified microscopy/spectroscopy platform, to explore the optical density of states of nanostructures as an example. Here, we discuss the interactions between light and free-electron wavepackets from first principles, by developing a simulation toolbox that combines Maxwell and Schrödinger equations [1, 2].

Results

Electron-light interactions in free-space, could be tuned to be either elastic or inelastic. Generalization of the so-called Kapitza-Dirac effect to the inelastic scattering is fulfilled by either incorporating various light beams of different colors [3] or structured light [4] (Fig. 1). In the case of near-field light, both elastic and inelastic contributions are observed [1], allowing for determining the strength of electron-light interactions by both diffraction and spectroscopy means. We further discuss the outlook for further generalizing the numerical technique for including the interaction of pre-shaped electron beams with light and quantum matter.

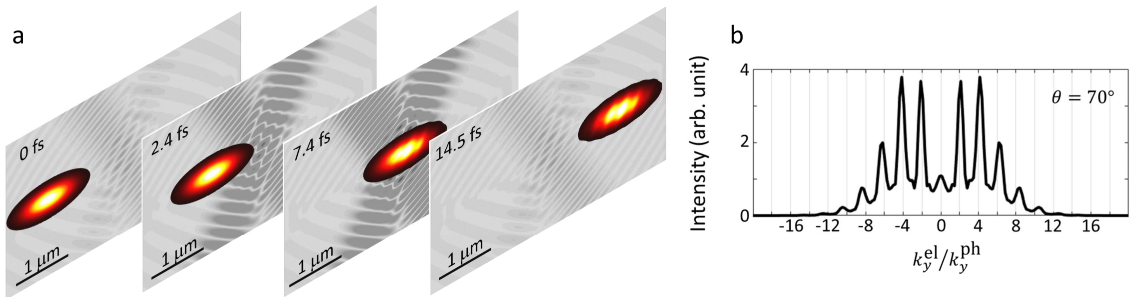

Fig. 1. (a) Interaction of an electron wavepacket with two optical Gaussian beams, where the distribution of the electron wavepacket (colored image) and light (electric field, grayscale) are shown at depicted times. (b) Lateral momentum distribution of the electron beam after the interaction.

References

[1] N. Talebi, *Phys. Rev. Lett.* 125, 080401 (2020).

[2] N. Talebi, *Advances in Physics: X* 3 (1), 1499438 (2018)

[3] M. Kozak, T. Eckstein, N. Schönenberger, P. Hommelhoff, *Nature Physics* **14**, 121–125 (2018)

[4] S. Ebel and N. Talebi, arXiv:2212.10255 (2023)

Open source finite element models for photonics with ONELAB/Gmsh/GetDP

G. Demésy
Aix Marseille Univ, CNRS, Centrale Marseille, Institut Fresnel, Marseille, France
guillaume.demesy@fresnel.fr

We present a library of full-featured models [1] for photonics that can be used "as is" for parametric studies or as templates for custom applications in photonics.

Introduction

We present a set of models for (nano)photonics [1] relying on Finite Elements and based on the open source softwares ONELAB [2], Gmsh [3] and GetDP [4] developped by C. Geuzaine (Université de Liège). The flexibility of Gmsh with its built-in CAD kernel and the versatility of GetDP, which supports high order (edge and nodal) elements and Bloch conditions, make them suitable candidates for many (nano)photonic applications. GetDP has been interfaced with the high performance library PETSc [5] for sparce matrix algebra, and more recently to the general SLEPc [6] eigenvalue solvers. Finally, the ONELAB interface allows to use the models in a black box manner, while advanced users can dive into the code and quite easily adapt it to suit their needs.

Summary

These softwares allowed the conception of very versatile models that will be presented :

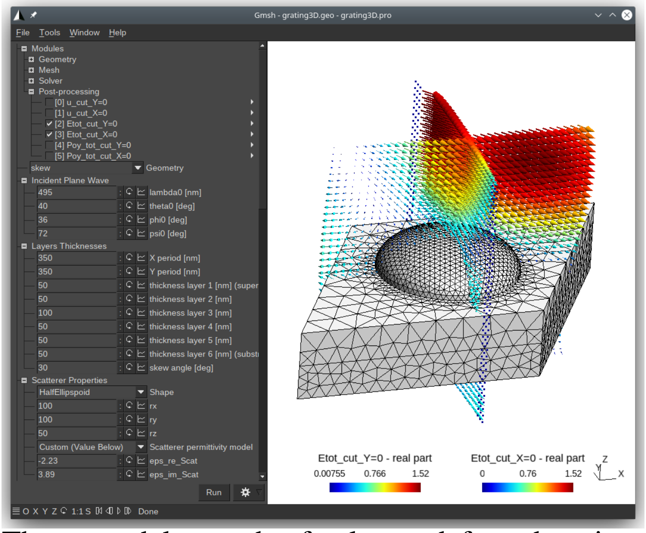

- diffraction gratings in 2D/2.5D/3D (figure opposite: A skewed lattice crossed grating)
- scattering by 3D objects
  - plane wave reponse
  - Green tensor
  - scattering matrix
  - Quasi-Normal Modes (QNMs)
- photonic crystal bandstructure
- waveguide leaky modes
- Dispersive Quasi-Normal Modes
- QNM expansion

These models can be freely used for educational purposes (they are currently deployed in Aix-Marseille Université for undergraduate students) or for research applications (they are currently installed on laptops and workstations in Institut Fresnel and on Aix-Marseille Université HPC facilities).

References

[1] See `http://onelab.info/photonics` and references therein.
[2] `http://onelab.info`
[3] C. Geuzaine and J.-F. Remacle. *International Journal for Numerical Methods in Engineering* 79(11), pp. 1309-1331, 2009.
[4] P. Dular, C. Geuzaine, F. Henrotte and W. Legros. *IEEE Transactions on Magnetics* 34(5), pp. 3395–3398, 1998.
[5] `https://petsc.org/`
[6] `https://slepc.upv.es/`

Modelling and engineering of the optomechanical coupling in subwavelength-structured silicon waveguides

Paula Nuño Ruano [1], Jianhao Zhang [1,2], Daniele Melati [1], David González-Andrade [1], Xavier Le Roux [1], Eric Cassan [1], Delphine Marris-Morini [1], Laurent Vivien [1], Norberto Daniel Lanzillotti-Kimura [1], Carlos Alonso-Ramos [1],

[1] *Centre de Nanosciences et de Nanotechnologies, Université Paris-Saclay, CNRS, France*

[2] *Present address: National Research Council Canada, Canada*

paula.nuno-ruano@c2n.upsaclay.fr

On-chip optomechanical interactions have a great potential for applications in communications, sensing and quantum processing. We combine multiphysics optomechanical simulations and automatic optimisation techniques to design subwavelength-nanostructured silicon waveguides achieving strong optomechanical coupling.

Introduction

The optomechanical Brillouin interactions can be greatly magnified by strong radiation pressure on the boundaries of suspended nanometric-scale silicon waveguides. Thus, subwavelength-structured designs appear as promising candidates for strong on-chip optomechanical coupling where the radiation pressure can be tailored and optimised.

Results

We develop nanostructured silicon waveguides that allow independent control of photonic and phononic modes to yield strong Brillouin gain [1]. We combine optical and mechanical simulations with a genetic algorithm to address the multiphysics, and multiparameter optimisation of the waveguide structure. Our optimised designs (fig. 1) yield remarkably high calculated gains, of $\sim 3000\ \mathrm{W}^{-1}\mathrm{m}^{-1}$ for high-frequency mechanical modes (up to 15 GHz), and near-infrared optical modes (with wavelengths –in vacuum– around 1550 nm) [2].

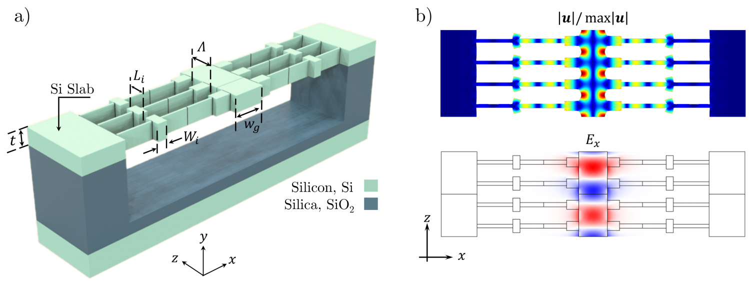

Fig. 1. a) One of the proposed subwavelength-structured silicon membranes yielding large Brillouin gain. b) Mechanical mode (up) and TE-optical mode (down) sustained by the geometry [2].

Conclusions

The multiphysics modelling and optimisation strategy presented here opens exciting new prospects for the development of high-performance optomechanical devices in silicon photonics technology.

References

[1] J. Zhang *et al.* Subwavelength engineering for brillouin gain optimization in silicon optomechanical waveguides. *Optics Letters*, 45(13):3717–3720, 2020.

[2] P. Nuño Ruano *et al.* Genetic optimization of brillouin scattering gain in subwavelength-structured silicon membrane waveguides. *Optics & Laser Technology*, 161:109130, 2023.

MAN: A freeware to compute and analysis modes of resonators

T. Wu[1,*], P. Lalanne[1]
[1]*LP2N, Institut d'Optique Graduate School, CNRS, Univ. Bordeaux, 33400 Talence, France*

* tong.wu@institutoptique.fr

In this talk, we introduce MAN (Modal Analysis of Nanoresonators) a software with many open scripts, which computes and normalizes the quasinormal modes (QNMs) of electromagnetic resonators.

Introduction

In this talk, we present MAN [1-2], an open-source software that uses the QNM basis for analyzing the response of virtually any resonators or antennas, be they composed of dispersive, anisotropic, or non-reciprocal materials, or operated at high (optical and near-IR waves) or low (RF waves) frequencies. MAN is conceived to educatively help the user analyze the physics of electromagnetic resonators towards the identification of the dominant QNMs to speed up the simulation of resonant structures and offer physical transparency in the design.

Result

Figure 1 shows the structure of the software. MAN is the result of a collective effort over the last decade. It gathers two solvers, QNMPole [3] and QNMEig [4], which have already acquired a good reputation as can be seen from the number of citations of the referent publications [3-4] or software downloads [2]. QNMEig provides a comprehensive interface to the commercial software COMSOL Multiphysics; QNMPole can be used with any software capable of solving Maxwell equations in the frequency domain. MAN additionally features many toolboxes that illustrate how to use the software for analyzing various emblematic geometries with a superposition of QNMs, therein providing a transparent interpretation of the physics.

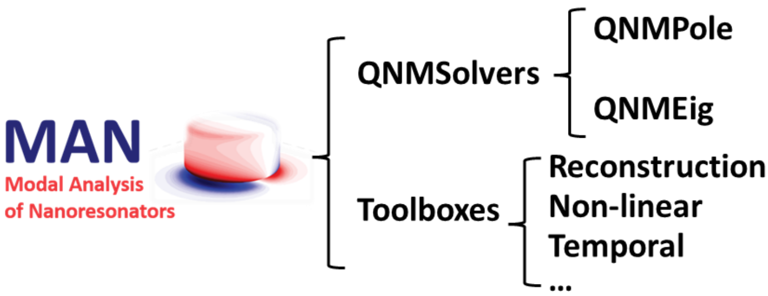

Fig. 1. Structure of MAN.

References

[1] T. Wu, D. Arrivault, W. Yan, P. Lalanne, Modal analysis of electromagnetic resonators: User guide for the MAN program, Comput. Phys. Commun., 284, 108627, 2023.

[2] https://doi.org/10.5281/zenodo.7400937

[3] Q. Bai, M. Perrin, C. Sauvan, J.-P. Hugonin, P. Lalanne, Efficient and intuitive method for the analysis of light scattering by a resonant nanostructure, Opt. Express, 21, 27371, 2013.

[4] W. Yan, R. Faggiani, P. Lalanne, Rigorous modal analysis of plasmonic nanoresonators. Phys. Rev. B, 97, 205422, 2018.

Coated Microtoroid versus Coated Microsphere for Biosensing Applications

M. Jalali[1,*], D. Erni[1]
[1] *General and Theoretical Electrical Engineering (ATE), Faculty of Engineering, University of Duisburg-Essen, and CENIDE – Center for Nanointegration Duisburg-Essen, 47048 Duisburg, Germany*
*mandana.jalali@uni-due.de

The role coated microresonator's shape – namely of a toroidal or spherical structure - on their biosensing limit is investigated. Results show that in aquatic media and hence for biosensing applications microspheres through adding a well-designed shell, show higher sensing limits compared to microtoroids.

Adding a well-designed shell to a given microresonator improves the resonator's sensing limit substantially, as the shell (from a material with higher refractive index compared to the microresonator) will increase the resonator's quality factor through reducing the radiation losses. It also shifts the mode toward the microresonator's surface and accordingly reduces the mode volume and improves the electric field intensity at the sensing location [1, 2]. A 150nm thick polystyrene (PS) shell is added to a 30µm silica microsphere as well as a silica microtoroid with 20µm/4µm major/minor axes, where the microresonators are located both in air and in an aquatic medium. The structures are modelled and simulated with the eigenmode solver of Comsol Multiphysics, determining the quality factors, mode volumes and normalized electric field intensities for both, the microtoroid and the microsphere with and without a 150nm PS shell in aquatic and air medium. Results show that, although microtoroids have prominently higher quality factors compared to microspheres, in aquatic media the quality factor of the microtoroid reduces only to 1.8×10^4 and the presence of the shell improves it to 3.1×10^4. However, in the case of the microsphere the shell improves the quality factor from 5.2×10^4 up to 2.4×10^5 and additionally, the mode volume reduces more than 20%, together with enhanced electric field intensity at the sensing area, namely the immediate vicinity if the microresonator. The electric field distribution of the excited whispering gallery mode in the case of microtoroid and microsphere in aquatic medium with and without the shell are illustrated in the Fig. 1. Accordingly, it can be concluded that a well-designed coated microsphere, is better suited in biosensing applications where the sensing occurs in aquatic media.

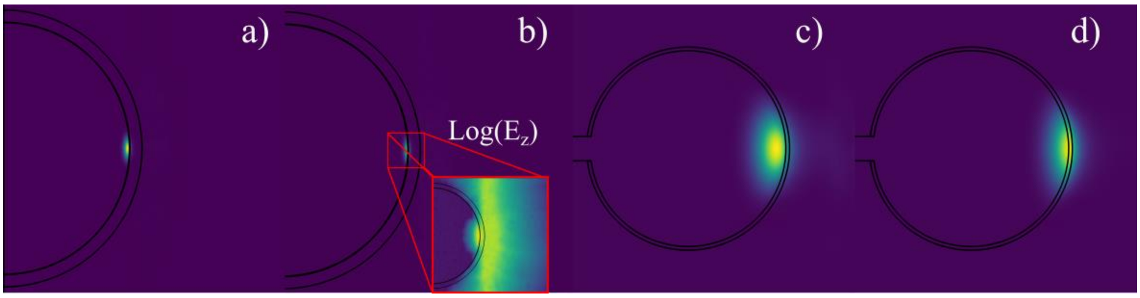

Fig. 1. The an azimuthal cross-section of the excited whispering gallery mode's electric field distribution for the cases of a) microsphere without shell, b) microsphere with shell – the inset depicts the excited mode in the logarithmic scale, c) microtoroid without shell, d) microtoroid with shell in aquatic medium.

References

[1] M. Jalali, and D. Erni, *Early stage, label-free detection of breast cancer based on exosome's protein content alteration*. Proc. SPIE 12139, Optical Sensing and Detection VII, 121390G, 2022.

[2] M. Jalali, N. Benson, and D. Erni, *Detecting protein alteration within an exosome by means of a coated dielectric microsphere resonator*, in [2021 Conference on Lasers and Electro-Optics Europe & European Quantum Electronics Conference (CLEO/Europe-EQEC)], 1–1, IEEE, 2021.

Numerical Demonstration of a Photonic Reservoir Computing Based on a Stimulated Brillouin Scattering System

S. Phang[1]
[1]George Green Institute for Electromagnetics Research, University of Nottingham, UK
*sendy.phang@nottingham.ac.uk

A new architecture of a photonic reservoir computing based on the stimulated Brillouin scattering phenomena is reported. The contribution will describe a methodology to calibrate such a system and report the performance of such system through machine learning benchmark tests. The contribution will allow the realisation of a new passive artificial intelligence (AI)-hardware system.

Introduction

A new class of photonic system called *Photonic Reservoir Computing* (PhRC) has emerged as a potential candidate for the development of hardware capable of performing AI [1]. The PhRC is a type of photonic system that is inspired by the architecture of the brain. It involves the development of photonic hardware systems that mimic the structure and function of human nervous system.

Methodology

In this contribution, a new architecture of a PhRC is introduced harnessing the chaotic wave behaviour of light in the presence of Brillouin scattering. Here, a stimulated-kind of Brillouin scattering (SBS) in an optical fibre system, which is modelled by the three-wave interaction (TWI) nonlinear coupled equations, is considered, i.e., PhRC-SBS system, see Fig. 1(left).

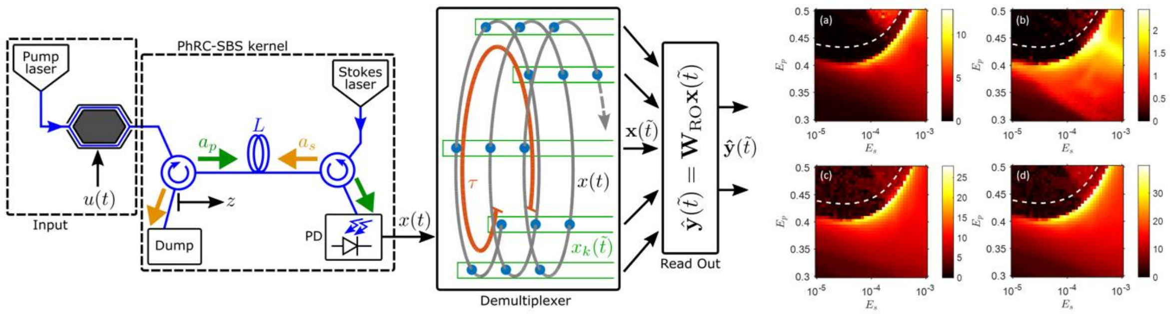

Fig. 1(Left) Schematic of the PhRC-SBS system. **(Right)** Memory capacity of an PhRC-SBS system: (a) Linear, (b) Nonlinear quadratic, (c) Nonlinear cross and (d) total memory capacities. Dashed line denotes the bifurcation line of the SBS-PhRC system.

Conclusion

By solving the TWI equations, a new application of stimulated Brillouin scattering for photonic reservoir computing (PhRC-SBS) is demonstrated. The contribution will show the benchmark performance of the PhRC-SBS in terms of its linear and nonlinear memory capacities and the error-rate in performing machine learning benchmarks. The memory capacities of the new PhRC-SBS passive system are comparable to other PhRC designs which uses active components. Furthermore, it will show that the performance of the SBS-PhRC system is strongly dependent on the chaotic nature of the SBS and further demonstrate that the optimum operation of such a system occurs at the edge of chaos. Figure 1(right) depict the total memory capacity of the PhRC-SBS system as a function of (normalised-value) electric fields. The highest memory capacities occur at distinct region near the bifurcation line.

References

[1] S. Phang, P. Sewell, A. Vukovic, TM Benson, *The Optical Reservoir Computer: a New Approach to a Programmable Integrated Optics System Based on an Artificial Neural Network*, Integrated Optics Volume 2: Characterization, devices and applications. Institution of Engineering and Technology, 2020.

Time-Delayed Photonic Reservoir Computing for Chemical Sensing: Numerical Model and Experimental Demonstrations

G. Anufriev[1], M. Farries[1], D. Furniss[1], S. Phang[1], A. Seddon[1].
[1]*George Green Institute for Electromagnetics Research, University of Nottingham, UK*
gleb.anufriev@nottingham.ac.uk

Photonic reservoir computing (PhRC) is a recent development in neuromorphic computing implemented as a photonic system. In this paper, we report a realistic numerical model to simulate a PhRC based on a time delayed electro-optical system and demonstrate its application to perform classification of chemical's absorption spectra.

Introduction

The human nervous system is an extremely advanced 'biological computational system', with over 99.9% of it dedicated to sensory processing [1]. Inspired by its efficiency, speed, and computing capability, a new subclass of machine learning algorithms referred to as reservoir computing. The PhRC is the implementation of the reservoir computing in a photonic technology platform.

Methodology

Our PhRC experimental setup is based on a time-delayed electro-optic (EO) system which previously was numerically demonstrated in [1]. The setup consists of three parts: a sensor, the EO-PhRC, and a read-out, See Fig. 1(a). The sensor provides spectral measurements of the sample, which is processed by the EO-PhRC. A linear estimator is applied at the read-out to infer potential relationships/patterns of the transformed spectral information.

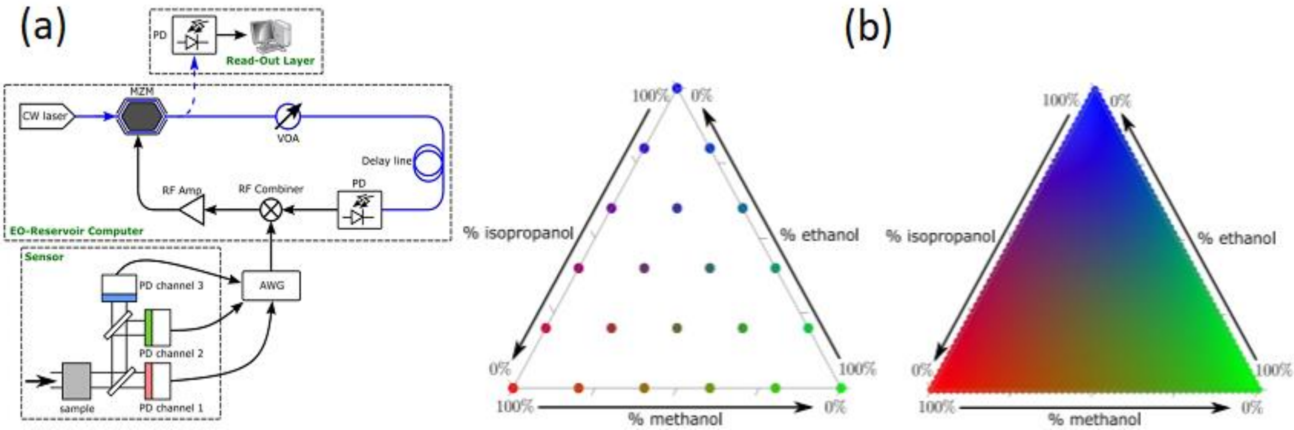

Fig. 1(a) The overall EO-PhRC based neuromorphic sensing device. (**b**) Numerical demonstration of the EO-PhRC for regression in chemical's absorption spectra identification.

Conclusion

A realistic numerical model has been developed and used to simulate the EO-PhRC for sensing application [1]. It is capable of performing a complex machine learning task of classification and regression based on chemical's absorption spectral dataset with high accuracy, as shown in Fig. 1(b). In this talk, we will report our experimental demonstration of such a setup.

References

[1] G. Anufriev, D. Furniss, M. Farries, S. Phang, *Non-spectroscopic sensing enabled by an electro-optical reservoir computer*, Opt. Mater. Express 12, 1767-1783 (2022)

Identifying extreme localization and rogue waves in fibre optics modulation instability using data-driven dominant balance

A.V. Ermolaev [1], M. Mabed [1], C. Finot [2], G. Genty [3], J.M. Dudley [1],
[1] *Université de Franche-Comté, Institut FEMTO-ST, CNRS, Besançon, France*
[2] *Université de Bourgogne, Laboratoire Interdisciplinaire Carnot de Bourgogne, CNRS, 21078 Dijon, France*
[3] *Photonics Laboratory, Tampere University, Tampere, FI-33104, Finland*
andrei.ermolaev@femto-st.fr

We use the Machine Learning (ML) technique of data-driven dominant balance to automatically identify local regions of dispersive and nonlinear interactions in a noise-seeded Modulation Instability (MI) dynamics.

We report a novel approach to interpret MI dynamics in optical fibre propagation, using a data-driven dominant balance ML technique [1] aimed at automatically identifying the physical processes driving different local propagation regimes. Specifically, we study the noise-seeded MI in the nonlinear Schrödinger equation (NLSE) written in normalised form as: $iu_\xi + \frac{1}{2}u_{\tau\tau} + |u|^2u = 0$, where ξ is distance, τ is comoving time, and u is the field envelope. Figure 1 (a), (b) shows the application of data-driven dominant balance to the analytic solutions for the Peregrine soliton (PS) and the Akhmediev breather (AB) (see caption for details), localized structures well-known to arise from MI [2].

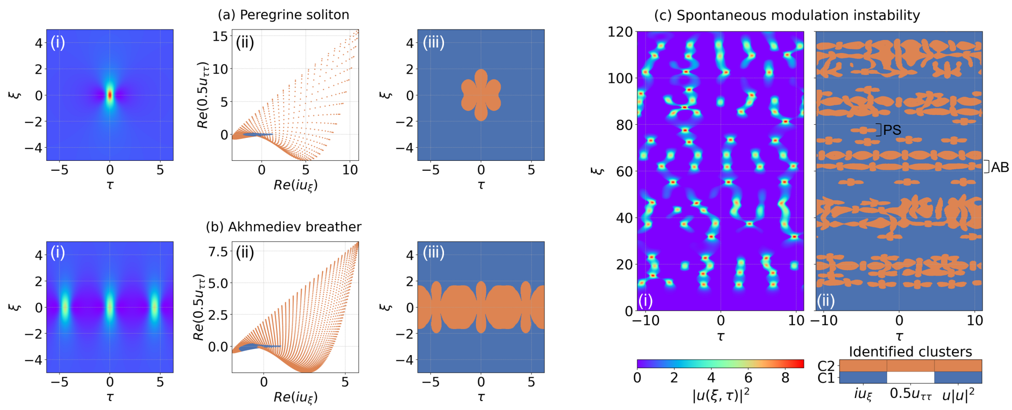

Fig. 1. (a) and (b) show dominant balance analysis for the PS and AB. First (i) the evolution map for $u(\xi,\tau)$ is defined; then (ii) by analysing the map in its "equation space" the clusters corresponding to different combinations of dominating NLSE terms (iu_ξ, $\frac{1}{2}u_{\tau\tau}$, $|u|^2u$) are identified; finally (iii) these clusters are remapped back to (ξ,τ) space for comparison with the evolution map. (c) displays the evolution map (i) and corresponding cluster map (ii) for the case of noise-seeded MI. The colormaps on the bottom right apply to all figures.

The key physical point evident in figures (iii) is that dispersion effects do not play a dominant role in the blue "continuous wave" region, in contrast to regions of strong temporal localisation (orange cluster) where dispersion contributes comparable to nonlinearity. These two regimes have been successfully distinguished even in a turbulent case of noise-seeded MI [see Figure 1(c)], demonstrating the power of the data-driven dominant balance to automatically assign interacting processes to particular stages of MI evolution and to provide additional insights into the arising physics. Obtained results suggest future applications in experimental analysis and data-driven discovery of physical laws [3].

References

[1] J.L. Callaham, J.V. Koch, B.W. Brunton, J.N. Kutz, and S.L. Brunton, *Learning dominant physical processes with data-driven balance models,* Nat. Commun. 12, 1016 (2021).
[2] J.M. Dudley, F. Dias, M. Erkintalo, and G. Genty, *Instabilities, breathers and rogue waves in optics,* Nat. Photon. 8, 755-764 (2014).
[3] A.V. Ermolaev, A. Sheveleva, G. Genty, C. Finot, and J.M. Dudley, *Data-driven model discovery of ideal four-wave mixing in nonlinear fibre optics,* Sci. Rep. 12, 12711 (2022).

Machine Learning analysis of Continuous Wave fiber Modulation Instability

M. Mabed[1,*], L. Salmela[2], A. Ermolaev[1], C. Finot[3] , G. Genty[2], J.M. Dudley[1]
[1] *Université de Franche-Comté, Institut FEMTO-ST, CNRS UMR 6174, 25000 Besançon, France*
[2] *Photonics Laboratory, Tampere University, Tampere, FI-33104, Finland*
[3] *Université de Bourgogne, Laboratoire ICB, CNRS UMR 6303, 21078 Dijon, France*
*mehdi.mabed@femto-st.fr

We use a neural network to explore temporal-spectral correlations in optical fiber modulation instability. We show in particular that any potential predictive power is very limited.

Introduction

Recent work has used machine learning in nonlinear fiber optics for fiber laser control, non-linear Schrödinger equation (NLSE) emulation, or prediction of temporal extreme events based only on spectral intensity analysis. These previous works have been performed on systems with higher order effects [1]. Here we report that such predictions can also be identified in ideal continuous wave MI.

Summary

We simulate the NLSE : $iA_z - \beta_2/2\ A_{TT} + \gamma|A|^2A = 0$ (β_2 = -21 ps^2 km^{-1} and γ = 1.1 W^{-1} km^{-1}) and use a 50 W noisy CW input to propagate over 545 km. After ~300 m the input evolves into fully-developed random MI, and we then extract spectral and temporal intensity profiles at 55 m intervals to form training and testing datasets. Fig. (a) shows typical profiles. We aim to correlate maximum temporal peaks P_k based on the corresponding spectra $S_k(\lambda)$. We use a feedforward neural network with hidden layers of 150 and 10 neurons. After training on 7500 spectral-temporal pairs, Fig. (b) shows validation results using 2500 simulations, for simulation-limited dynamic range of ~100 dB. We have studied if the network can predict the emergence of high intensity temporal peaks based on analyzing spectra at an earlier propagation distance from that at which the temporal peak intensity is extracted. Fig. (c) plots the correlation coefficient as a function of Δz, the distance between the spectra used as input to the network and the target temporal peak, for two different dynamic ranges.

Results

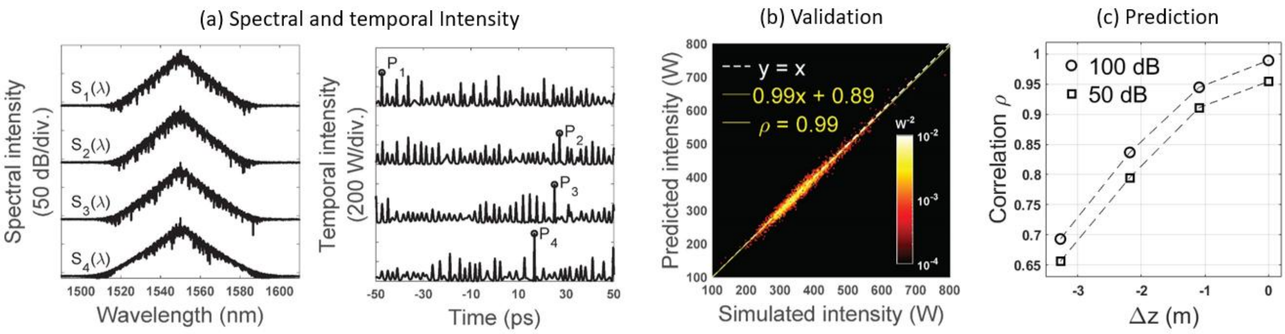

Fig. 1. (a) Four spectral and temporal profiles from CW modulation instability where we predict temporal peaks P_k from spectral intensity $S_k(\lambda)$. (b) Validation results for input dynamic ranges of 100 dB. (c) Correlation dependence on distance, where we try to correlate temporal peaks at a distance *z* with the spectral intensity at an earlier distance $z+\Delta z$.

Conclusion

Although correlation rapidly falls with distance, we establish limits on the useful ($\rho > 0.8$) predictive power of the network as associated with a distance of $\Delta z \sim 0.1 L_{NL}$. These results confirm the ability of neural networks to correlate temporal and spectral characteristics, and provide further insight into the use of neural networks in predicting dynamics in NLSE systems.

References

[1] G. Genty et al. Nature Photonics **15**, 91 (2021) ; L. Salmela *et al.* Nature Mach. Int. **3**, 344 (2021) ; L. Salmela et al. Opt. Lett. **47**, 802 (2022) ; Mabed *et al.* Opt. Express **30**, 15060 (2022)

Recent advances in Modelling Photonic Crystal Surface Emitting Lasers (PCSELs) Using Unstructured Transmission Line (UTLM) Modelling Method

A.Vukovic[1,*], B. Lang[1], P. Sewell[1]

S. Rihani[2], K. Boylan[2], G. Berry[2], N. Hattasan[2], D. Moodie[2], J. Rawsthorne[2]

[1]*George Green Institute for Electromagnetics Research, Faculty of Engineering, University of Nottingham, Nottingham, United Kingdom*

[2]*Huawei Technologies Research and Development, Ipswich, United Kingdom*

*ana.vukovic@nottingham.ac.uk

Introduction

Photonic Crystal Surface Emitting Lasers (PCSELs) are promising candidates for the realization of single mode, high power and high brightness lasers [1,2]. To improve the output power, beam shape and intensity, a number of InP based PCSEL designs have been demonstrated including single lattice PCSELs with triangular scatterers and double lattice PCSELs comprising ellipsoidal and circular scatterers [1,2]. Despite significant experimental demonstrations of PCSEL performance, very few direct comparisons between the theoretical and experimental data are available in literature. We report on a fast and efficient methodology for simulating both double and single lattice PCSEL design and compare them with experimental results in order to develop a better understanding on how the shape and depth of the scatterers and the size of PCSEL affects the mode separation at the Γ point, the Q-factors of modes and the far field shapes and intensities.

Summary

Fast modelling approaches are important for quick exploration of a design space. For this purpose we adopt a methodology that assumes that the field in the 3D PCSEL structure is separable and can be expressed as product of the 2D transversal field distribution, $E_{2D}(x,y)$, and lateral 1D field distribution, $E_{1D}(z)$. A slab solver is used to obtain the slab profile of the lateral structure which is then weighted by the magnitude of the electric field to obtain effective indices of the scatterers and holes of the equivalent 2D PC structure. The density of $|E_{2D}|^2$ is then used to update the effective index of the PC layer in the slab solver. This approach is iterated until the method converges. Comparisons between experimental and predicted data show that this methodology agrees better with experimental results compared to the simple effective index approach as it also accounts for the depth of the scatterers. The presentation will expand on the methodology, discuss the impact of numerical discretization and the shape of the scatterers and double lattice separations. Comparisons with 3D simulations and experiments will also include far field shape and intensity.

References

[1] M. Yoshida, M. D. Zoysa, K. Ishizaki, Y. tanaka, M. Kawasaki, R. Hatsuda, B. Song, J. Gelleta, S. Noda, "*Double-lattice photonic-crystal resonators enabling high-brightness semiconductor lasers with symmetric narrow-divergence beams*", Nature Materials, Vol.18. pp.121-128, 2019.

[2] Y. Itoh, N. Kono, D. Inoue, N. Fujiwara, M. Ogasawara, K. Fujii, H. Yoshinaga, T. Inoue, M.D. Zoysa, K. Ishizaki, S. Noda "*High-power CW oscillation of 1.3 mm wavelength InP-based photonic crystal surface emitting lasers*", Optics Express, Vol30. No.16, 2022.

FETI method applied to the scattering studies of long resonant structures

H. Tortel, A.-L. Fehrembach
Aix Marseille Univ, CNRS, Centrale Marseille, Institut Fresnel, 13013 Marseille, France.

In this paper we will present the application of a domain decomposition technique to the study of the electromagnetic scattering of cavity resonant gratins which are highly resonant structures with a subwavelength pattern and a total length around hundreds of wavelengths.

Summary :

The need of engineering simulations of large and complex structures is rapidly growing, requiring numerical methods which are more and more efficient. As such, the Finite Element Method (FEM) applied to the resolution of time harmonic electromagnetic wave scattering has become very popular over the past decades.

In this method, the unknown of interest (the electric or magnetic field) is expanded onto a set of basis functions. A linear system is then calculated by projecting the Helmholtz equation onto the same set of test functions, as advocated by the Galerkin method. Thus, the efficiency of the method is mainly dependent upon one's own ability to solve the resulting sparse linear system, which can be time and memory consuming, especially in three-dimensional (3D) configurations.

Among the different schemes proposed to solve large scale models and preserve the versatility of the FEM method, the Domain Decomposition Method (DDM) and its different evolutions are especially appealing. The closely related Finite Element Tearing and Interconnecting (FETI) method seems also very robust when one is dealing with arbitrarily mesh partitions. The general principle of FETI methods is first to divide the entire computational domain into smaller non-overlapping subdomains. In each of these subdomains, local linear systems can now more easily be inverted. Simultaneously, the different adjacent subdomains are glued at their common interfaces thanks to appropriate boundary conditions, leading to a so-called global interface problem.

Once this interface problem is solved, the solution inside each subdomain can be evaluated independently by using the known mixed boundary conditions at the internal interfaces between subdomains. In this paper we propose to study the performances of this method when we apply it to the modelling of highly resonant structures which are subwavelength patterned and with a total length around hundreds of wavelengths.

Acknowledgements: this work was supported by the AID (ANR-ASTRID RESON project).

[1] Javad Moshfegh A Parallel Direct Method for Finite Element Electromagnetic Computations Based on Domain Decomposition, PhD Thesis 2019.
[2] Anne-Laure Fehrembach, François Renaud, Evgeny Popov, Herve Tortel, Antoine Monmayrant, Olivier Gauthier-Lafaye, and Stephane Calvez. Dark mode-in-the-box for enhanced second harmonic generation in corrugated waveguides. Optics Ex- press, 29(25) :40981, November 2021

Full Vectorial 3-D Non-Paraxial Beam Propagation Method

Pratiksha Choudhary[1], Anurag Sharma[1,2]
[1]*Department of Physics, Indian Institute of Technology Delhi, New Delhi, 110016, India*
[2]*Optics & Photonics Centre, Indian Institute of Technology Delhi, New Delhi, 110016, India*[1]phz188425@iitd.ac.in; [2]asharma@iitd.ac.in

We present a full vectorial non-paraxial (wide-angle) 3-D propagation method based on finite-difference method. Examples on silicon and silicon nitride waveguides are included.

Introduction to the Method

Paraxial approximation has been commonly used for developing beam propagation methods (see *e.g.* [1]). We had earlier developed a non-paraxial scalar propagation method for wide-angle propagation [2]. The method was based on symmetrized splitting of the non-paraxial propagation operator. We have now extended the same concept to the full vectorial wave equation. There have been ways to go beyond the paraxial iteratively using Pade' approximants [3] with limited success. Finite difference time domain (FDTD) methods are generally employed for full vectorial propagation, but these are computationally intensive, particularly for 3-D problems. Our method can be used to propagate a given incident wave, *e.g.*, a mode, through a given structure. Further, in our method, the splitting of the propagation operator can be tailored to improve the stability and efficiency of propagation.

Results

As a numerical example, we consider the example involving the propagation of the fundamental mode of a rectangular silicon waveguide. The waveguide has a width of 500nm, and a height of 220nm, with refractive indices of core and cladding, respectively, are n_{core}=3.5(silicon) and n_{clad}=1(air) and a wavelength of 1500nm. Figure (a) shows the field at the y=0 line after propagation through 100 μm for a silicon rectangular waveguide and Fig. (b) shows a plot of error versus propagation distance for different propagation step length, Δz. As a measure of accuracy, we computed the error in terms of correlation factor between the modal field before and after propagation. Figure (c) shows a comparison of time taken by regular splitting of operator and an alternative splitting; the latter being much faster. More results will be presented at the Workshop.

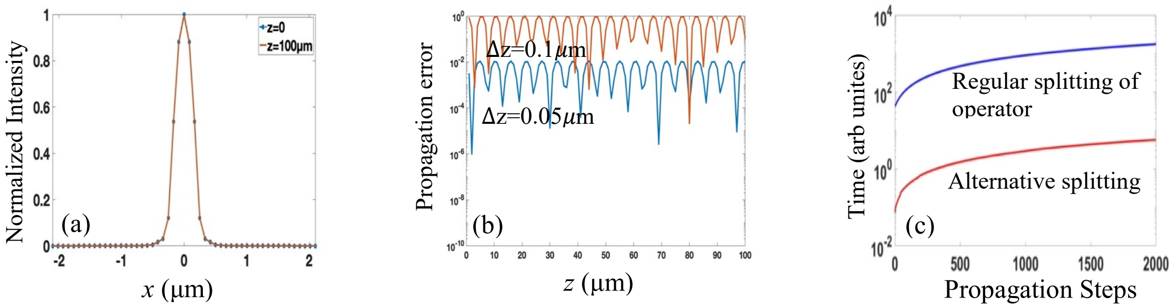

Work partially supported by UGC fellowship to P. Choudhary & SERB J.C. Bose fellowship to A. Sharma.

References

[1] W.P. Huang and C.L. Xu, "*Simulation of three-dimensional optical waveguides by a full-vector beam propagation method*," IEEE J. Quantum Electron. **29**, 2639-2649 (1993).
[2] D. Bhattacharya and A. Sharma, "*Split step non-paraxial finite difference method for 3D scalar wave propagation,*" Opt. Quantum Electron. **39**, 865-876 (2007).
[3] D. Yevick, Jun Yu, W. Bardyszewski, M. Glasner, "*Stability issues in Vector electric field propagation,*" IEEE Photon. Technol. Lett., **7**, 658-660 (1995).

No circular birefringence exists in a chiral medium

Zhi-Juan Hu[1], Chun-Fang Li[2,*]
[1]*Department of Physics, Shanghai Normal University, 100 Guilin Road, 200233 Shanghai, China*
[2]*Department of Physics, Shanghai University, 99 Shangda Road, 200444 Shanghai, China*
*cfli@shu.edu.cn

A logical analysis shows that the circular birefringence, which was assumed in 1825 by Fresnel to describe the optical activity in a chiral medium, does not exist.

Introduction

Circular birefringence refers to different propagation speeds or different indices of refraction [1] for right-handed and left-handed circularly-polarized waves in a chiral medium. Due to the observation of the phenomenon of circular double refraction at the surface of a chiral medium, as implemented by Ghosh and Fischer [2], circular birefringence seems to have been widely accepted as true. However, the assumption of circular birefringence makes the propagation speed of a linearly-polarized wave in a chiral medium become problematic. In solving this problem with a logical analysis, we find that it does not hold.

A logical analysis

The electric fields of right-handed and left-handed circularly-polarized plane waves propagating along the z-axis in an isotropic chiral medium can be written as [3]

$$\mathbf{E}_{+,t} = \left\{(\bar{x} + i\bar{y})/\sqrt{2}\right\} TE_i \exp(ik_{+,t} z), \quad \mathbf{E}_{-,t} = \left\{(\bar{x} - i\bar{y})/\sqrt{2}\right\} TE_i \exp(ik_{-,t} z),$$

respectively, where the time-dependence $\exp(-i\omega t)$ is assumed, $\bar{x}$ and $\bar{y}$ are unit vectors along the corresponding axes, TE_i is the amplitude, $k_{+,t} = k - \tau$, and $k_{-,t} = k + \tau$. As is well known, the superposition of $\mathbf{E}_{+,t}$ and $\mathbf{E}_{-,t}$ gives rise to the following rotatory linearly-polarized wave,

$$\mathbf{E}_{1,t} = (\mathbf{E}_{+,t} + \mathbf{E}_{-,t})/\sqrt{2} = (\bar{x}\cos\tau z + \bar{y}\sin\tau z) TE_i \exp(ikz).$$

But at the same time, their superposition can also yield another rotatory linearly-polarized wave,

$$\mathbf{E}_{2,t} = -i(\mathbf{E}_{+,t} - \mathbf{E}_{-,t})/\sqrt{2} = (\bar{y}\cos\tau z - \bar{x}\sin\tau z) TE_i \exp(ikz),$$

which is orthogonal to $\mathbf{E}_{1,t}$ at the same propagation distance z. It follows that whether $\mathbf{E}_{+,t}$ or $\mathbf{E}_{-,t}$ can be represented as a superposition of $\mathbf{E}_{1,t}$ and $\mathbf{E}_{2,t}$,

$$\mathbf{E}_{+,t} = (\mathbf{E}_{1,t} + i\mathbf{E}_{2,t})/\sqrt{2}, \quad \mathbf{E}_{-,t} = (\mathbf{E}_{1,t} - i\mathbf{E}_{2,t})/\sqrt{2}.$$

Results

Since the two linearly-polarized waves must propagate at the same speed, the two circularly-polarized waves should propagate at the same speed as the linearly-polarized waves. Circular double refraction [2] reflects the opposite phases [3] that the two circularly-polarized waves acquire as they rotate in the same way as the linearly-polarized waves.

Conclusion

It is thus concluded that there is no circular birefringence in an isotropic chiral medium.

References

[1] D. H. Goldstein, Polarized Light, 3rd ed. (Taylor and Francis, New York, 2011).
[2] A. Ghosh, P. Fischer, Phys. Rev. Lett. **97**, 173002 (2006).
[3] Z.-J. Hu, C.-F. Li, New J. Phys. **25**, 023007 (2023).

Anisotropy engineered metamaterials for polarization and mode management in integrated photonics

José Manuel Luque-González[1*], Pavel Cheben[2], Robert Halir[1,3], Pablo Ginel-Moreno[1], Alejandro Sánchez-Postigo[1,4], Abdelfettah Hadij-ElHouati[1,5], J. Gonzalo Wangüemert-Pérez[1,3], Jens H. Schmid[2], Íñigo Molina-Fernández[1,3] and Alejandro Ortega-Moñux[1]

[1]*Telecommunication Research Institute (TELMA), Universidad de Málaga, CEI Andalucía TECH, Louis Pasteur 35, 29010 Málaga, Spain*

[2]*National Research Council Canada, 1200 Montreal Road, Bldg. M50, Ottawa K1A 0R6, Canada*

[3]*Bionand Center for Nanomedicine and Biotechnology, Parque Tecnológico de Andalucía, 29590 Málaga, Spain*

[4]*Currently MSCA Postdoctoral Fellow at WWU Münster, Germany,*

[5]*Currently Photonic design engineer at Ligentec SA, Switzerland*

*jmlg@ic.uma.es

(Invited)

Abstract

Subwavelength grating (SWG) metamaterials have opened up new degrees of freedom in integrated photonics, enabling the development of nanophotonic devices with unprecedented performance. In this presentation, we review our recent advances in anisotropy engineered SWG metamaterial devices for silicon photonics.

Summary

SWG metamaterials are optical nanostructures comprising a spatial array of subwavelength-scale elements. By manipulating the shape, size, and period of the nanostructure, the optical properties of the material can be tailored to achieve specific functionalities, including wavefront shaping, polarization manipulation and spectral filtering [1-3]. In this presentation, we present an overview of our recent advances in anisotropic engineered SWG metamaterials designed to enhance the performance of state-of-the-art silicon photonic devices, including nanophotonic couplers, spectral filters, polarization control devices, wavelength multiplexers and optical nanoantennas.

References

[1] P. Cheben, R. Halir, J. H. Schmid, H. A. Atwater, and D. R. Smith, "Subwavelength integrated photonics," Nature 560, 565–572 (2018).

[2] R. Halir, A. Ortega-Moñux, D. Benedikovic, G. Z. Mashanovich, J. G. Wangüemert-Pérez, J. H. Schmid, Í. Molina-Fernández, and P. Cheben, “Subwavelength-grating metamaterial structures for silicon photonic devices,” Proc. IEEE 106, 2144–2157 (2018).

[3] J. M. Luque-González, A. Sánchez-Postigo, A. Hadij-ElHouati, A. Ortega-Moñux, J. G. Wangüemert-Pérez, J. H. Schmid, P. Cheben, Í. Molina-Fernández, and R. Halir, "A review of silicon subwavelength gratings: building break-through devices with anisotropic metamaterials," Nanophotonics 10, 2765–2797 (2021).

The comb waveguide: a new tool for WaveguideQED

N. Fayard [1], A. Bouscal [2], J. Berroir [2], A. Urvoy [2], T. Ray [2], S. Mahapatra [3], M. Kemiche [3], J.-A. Levenson [3], J.-J. Greffet [1], K. Bencheikh [3], J. Laurat [2], C. Sauvan [1]

[1] *Université Paris-Saclay, Institut d'Optique Graduate School, CNRS, Laboratoire Charles Fabry, 91127 Palaiseau, France*

[2] *Laboratoire Kastler Brossel, Sorbonne Université, CNRS, ENS-Université PSL, Collège de France, 4 place Jussieu, 75005 Paris, France*

[3] *Centre de Nanosciences et de Nanotechnologies, CNRS, Université Paris-Saclay, 91120 Palaiseau, France*

fayardnikos@gmail.com

1

Coupling cold atoms and nanostructured waveguides has triggered the emergence of a new field of research known as waveguide QED (WQED). In this work, we design a comb waveguide that provides strong interactions between atoms and guided photons with an unusual dispersion and a beta factor as high as 0.88 [1].

Photons travelling through waveguides can carry efficiently the quantum information while atoms trapped in its vicinity can store it for long times. This is the basic idea that lead to the emergence of WQED that reach its full potential of applications when the decay rate of the atoms inside the waveguide mode $\Gamma_{1\text{D}}$ exceeds greatly the decay into every other modes Γ'. A promising route to reach this regime is to use periodic dielectric waveguides. Indeed, since $\Gamma_{1\text{D}} \propto n_g$ (the group index of the mode [2]), it theoretically tends towards ∞ close to a band edge pushing the $\beta = \frac{\Gamma_{1\text{D}}}{\Gamma_{1\text{D}}+\Gamma'}$ factor close to unity. The Alligator waveguide [3] was built upon this idea. However, it has two major flaws: a lack of accessibility of the trapping region and a very curved dispersion of the slow mode not robust enough against disorder in fabrication. Thus, only $N = 3$ atoms have been trapped close to this structure, with a moderate coupling to the slow mode $\Gamma_{1\text{D}} \sim \Gamma'$ ($\beta = 0.5$).

To improve those figures of merits, we designed an asymetric comb waveguide [1] with the following assets: 1- the atoms can be trapped in the back of the structure where the accessibility is maximal, leading to a value of $\beta = 0.88$. 2- the transverse asymmetry of the structure provides additional degrees of freedom to engineer the dispersion curve[4]. We designed a completely new quartic dispersion $\omega \sim \Delta k^4$, that provides more resilience to our structure against fabrication imperfections and enlarges its operation bandwidth.

The fabrication of the comb waveguide is now in progress at C2N. We believe that the trapping of $N \sim 10-20$ atoms with a strong coupling to the comb waveguide can be seriously considered. Such high figures of merit would lead to the emergence of new physical phenomena. First, the quartic dispersion of the slow mode can drastically modify the collective effets that emerges when many atoms are strongly coupled to the structure. Second, thanks to the unprecedented value of $\beta = 0.88$ accessible with the comb waveguide, new quantum-non linear effects could be observed [5, 6] .

References

[1] N. Fayard et al., Optics Express 30 (25), 45093-45109, (2022).
[2] G Lecamp et al., Phys. Rev. Lett. 99(2), 023902 (2007).
[3] A. Goban et al., Physical Review Letters, **6**, 063601 (2015)
[4] H. S Nguyen et al., Phys. Rev. Lett. 120(6), 066102 (2018)
[5] N. Fayard et al., Physical Review Research, **4**, 023026 (2022)
[6] D. E Chang et al., Nat. Photonics 8(9), 685–694 (2014).

Approximation methods for the fast calculation of transmission of photonic wire bonds

M. Paszkiewicz [1], M. Sukhova [2], Y. Bao [3], W. Dörfler [2], C. Koos [3], C. Rockstuhl [2,4]

[1] *Institut für Theoretische Festkörperphysik (TFP), Karlsruhe Institute of Technology, Germany*
[2] *Institut für Angewandte und Numerische Mathematik (IANM), Karlsruhe Institute of Technology, Germany*
[3] *Institute of Photonics and Quantum Electronics (IPQ), Karlsruhe Institute of Technology, Germany*
[4] *Institut für Nanotechnologie (INT), Karlsruhe Institute of Technology, Germany*
maria.paszkiewicz@kit.edu

Photonic wire bonds are freeform dielectric waveguides that connect optical chips made of different materials in fully integrated photonic devices at a microscopic scale [1]. Here, we present an approximate method for the fast calculation of transmission, which has practical applications for the accelerated design of the wire bonds.

Summary

Simplified methods are favourable for the fast modelling of large optical structures, for which a numerical solution to Maxwell's equations is no longer feasible. In this work, we present a fundamental mode approximation (FMA) based on [2] and its extension to multi-mode approximation (MMA) to describe the light propagation in curved waveguides. The latter method intends to overcome limitations of the fundamental mode approximation when the waveguides support multiple modes [3]. As the example here, the methods are benchmarked with numerical simulations performed with Lumerical (FDTD). In spatial regions with a sudden change in the radius of curvature, light is coupled with a notable amplitude to these higher-order modes (Fig. 1 (left)), which affects the transmission of the fundamental mode (Fig. 1 (right)).

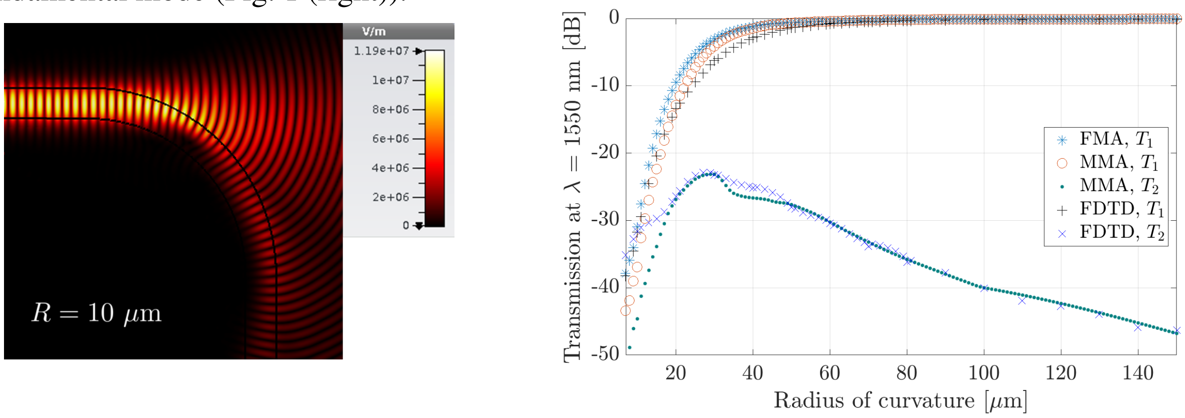

Fig. 1.: Magnitude of the instantaneous electric field in a dielectric waveguide of a straight-bend-straight form upon considering the fundamental mode of a straight waveguide as the illumination (left). Comparison of corresponding power transmitted in fundamental mode T_1 and second higher order mode T_2 as a function of radius of curvature (right).

References

[1] M. Blaicher, M. R. Billah, J. Kemal, T. Hoose, P. Marin-Palomo, A. Hofmann, Y. Kutuvantavida, et al. Hybrid multi-chip assembly of optical communication engines by in situ 3d nano-lithography. *Light: Science & Applications*, 9(1):71, 2020.

[2] F. Negredo, M. Blaicher, A. Nesic, P. Kraft, J. Ott, W. Dörfler, C. Koos, and C. Rockstuhl. Fast and reliable method to estimate losses of single-mode waveguides with an arbitrary 2d trajectory. *JOSA A*, 35(6):1063–1073, 2018.

[3] A. Nesic, M. Blaicher, E. Orlandini, T. Olariu, M. Paszkiewicz, F. Negredo, P. Kraft, M. Sukhova, A. Hofmann, W. Dörfler, et al. Transformation-optics modeling of 3d-printed freeform waveguides. *Optics Express*, 30(21):38856–38879, 2022.

A Propagation Method for Higher Order Modes in Fiber Structures

Ajay Kumar[1] and Anurag Sharma[1,2]
[1]*Department of Physics, Indian Institute of Technology Delhi, New Delhi, 110016, India*
[2]*Optics & Photonics Centre, Indian Institute of Technology Delhi, New Delhi, 110016, India*
[1]phz188359@iitd.ac.in; [2]asharma@iitd.ac.in

We present a method for propagation of scalar higher order modes (HOMs) in azimuthally symmetric structures. It is based on the collocation method and can be implemented for both paraxial and non-paraxial propagation. The method can be used to analyze structures like FBGs, Bragg fibers and ring core fibers.

Introduction to the Method

The fiber structures that retain azimuthal symmetry preserve the azimuthal variation of the field and the radial variation only need to be solved to obtain the propagated field. This reduces the computational effort greatly as has been shown earlier for LP_{0m} modes [1]. For higher order modes, the radial part for a given azimuthal symmetry is solved using the collocation method [2] using the appropriate associated Laguerre-Gauss functions as the basis functions. To solve the resulting collocation equation, we have implemented both paraxial [2] and non-paraxial [1] propagation methods. Using the former, we can model the problems involving non-reflecting structures such as Bragg fibers, ring-core fibers, LPGs and fiber tapers. Structures involving reflections such as FBGs require the use of non-paraxial propagation method. We present here examples of both types of structures. Leakage loss in a leaky structure such as a Bragg fiber can also be computed with this method and is presented in a separate companion paper.

Results

As an example, we propagate LP_{01} and LP_{11} modes in a few mode fiber Bragg grating [3]. The transmission spectrum is shown in Fig.(a) showing two distinct dips for the two modes. As an example of a longitudinally varying non-reflecting structure we consider a tapered ring core fiber [4]. A 8-mode fiber core is reduced by a factor of 2 such that higher order modes are cutoff. The power loss for various modes is shown in Fig.(b). More results will be presented at the Workshop.

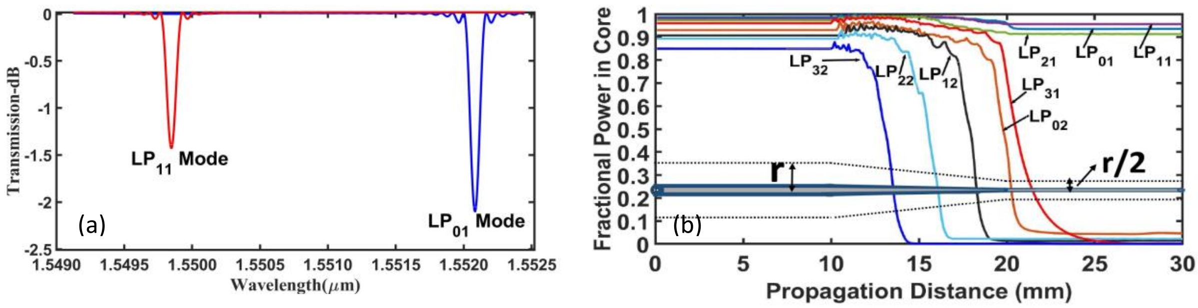

Work partially supported by CSIR fellowship to A. Kumar & SERB J.C. Bose fellowship to A. Sharma.

References:

[1]. R. Kumar, A. Sharma, "*A new method to analyze fiber Bragg gratings*," Opt. Fiber Technol. **53**, 102017 (2017).
[2]. A. Sharma, "*Collocation method for wave propagation through optical waveguiding structure*," Prog. Electromagn. Res. **11**, 143-198 (1995).
[3]. Li Yan *et al.* "*Characteristic analysis of two-mode fiber Bragg grating*," Appl. Phys. *B* **117,** 1221-1228 (2014).
[4]. M. Kasahara *et al.*, "*Design of Three-Spatial-Mode Ring-Core Fiber,*" J. Lightwave Technol. **32**, 1337-1343 (2014).

Beam Propagation Analysis for Bragg Fibers

Ajay Kumar[1,] and Anurag Sharma[1,2]
[1]*Department of Physics, Indian Institute of Technology Delhi, New Delhi, 110016,India*
[2]*Optics &Photonics Centre, Indian Institute of Technology Delhi, New Delhi, 110016, India*
[1]phz188359@iitd.ac.in; [2]asharma@iitd.ac.in

We present a method for analyzing Bragg fibers and computing leakage modal loss using the beam propagation method that we have developed for such azimuthally symmetric structures. We also optimize the layer thicknesses to maximize the fractional power in the core over a broader pass band.

Introduction

A Bragg fiber is made of alternating layers of low and high index material with the thickness determined by a mathematical equation involving the Bessel function [1]. The thickness of the layers is usually taken as uniform for a finite number of layers as an approximation [2]. In our method, we obtain the mode of such a fiber and propagate it using the method that we have developed for azimuthally symmetric structures. The method is based on the collocation method [3,4] using scaled Laguerre Gauss basis functions. Using this procedure, we have obtained the fraction of power in the core as a function of wavelength. This gives the pass band of the Bragg fiber. We have started with uniform thickness bilayers and then have optimized the thickness of bilayers to obtain wider pass band. We have found that only first 2-3 bilayers have to be optimized and other layers remain uniformly thick.

Results

As an example, we consider a Bragg fiber designed for 1.05μm wavelength [2] with nine bilayers of high and low refractive index. By optimizing the layer thicknesses, fractional power in the core is increased from 92.25% to 93.46% and the lower end of passband is now extended to 949nm instead of 962nm. The method can be used to analyze longitudinally varying fiber also and some examples will be presented at the workshop.

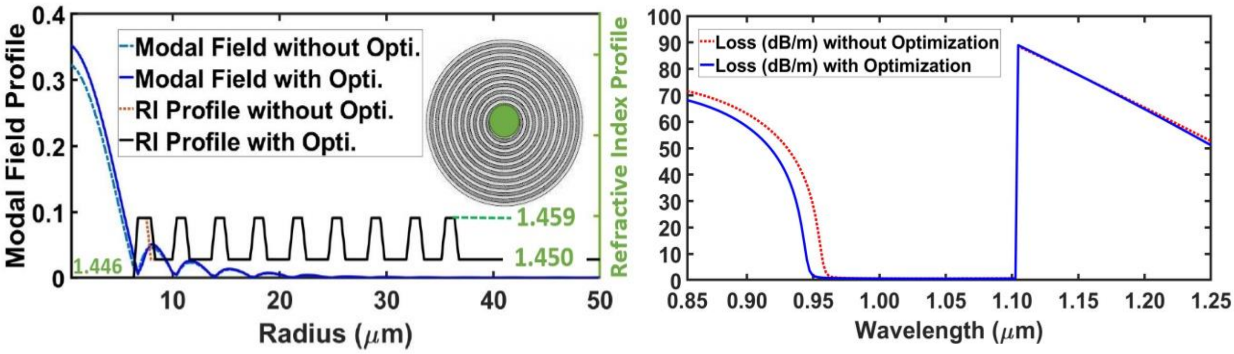

Fig. (a) Modal Field with & without Optimization (b) Loss (dB/m) with wavelength

Work partially supported by CSIR fellowship to A. Kumar & SERB J.C. Bose fellowship to A. Sharma.

References

[1] P. Yeh, A. Yariv and E. Marom, "*Theory of Bragg fiber*," J. Opt. Soc. Am. **68**, 1196 (1978).
[2] G.S. Kliros, "*Analysis of complex refractive index solid-core Bragg fibers*," Optoelectron. Adv. Mater. Rapid Commun. **3**. 309-312 (2009).
[3] A. Sharma, "*Collocation method for wave propagation through optical waveguiding structure*," Prog. Electromagn. Res. **11,** 143-198 (1995).
[4] A. Sharma and A. Taneja, "*Unconditionally stable procedure to propagate beams through optical waveguides using the collocation method*," Opt. Lett. **16,** 1162-1164 (1991)

SiGe photonics circuits for the mid-IR wavelength range

D. Marris-Morini[1], N. Koompai[1], T. H. N. Nguyen[1], V. Turpaud[1], V. Falcone[2], J. Frigerio[2], A. Ballabio[2], J.R. Coudevylle[1], D. Bouville[1], C. Villebasse[1], C. Alonso Ramos[1], L. Vivien[1], G. Isella[2]

[1] *Université Paris-Saclay, CNRS, Centre de Nanosciences et de Nanotechnologies, 91120 Palaiseau, France*
[2] *L-NESS, Dipartimento di Fisica, Politecnico di Milano, Polo di Como, Via Anzani 42, 22100 Como, Italy*

*delphine.morini@universite-paris-saclay.fr

Recent works on the development of graded-SiGe photonic integrated circuits for mid-IR photonics will be presented.

Optical spectroscopy in the mid-infrared (mid-IR) range is an unambiguous way to detect environmental and toxic analytes. Therefore, mid-IR photonics is of a great importance for many applications in sensing, imaging or even telecommunication. A challenging task is to make mid-IR spectroscopy accessible in remote areas, driving the development of compact and cost-effective solutions. The development of mid-IR photonics circuits has thus witnessed a burst of research activity in the recent years. Interestingly, germanium (Ge) based devices benefit from both the compatibility with large scale fabrication tools and a wide transparency window, extending up to 15 µm wavelength. In this context, recent works on the development of graded-SiGe photonic integrated circuits will be presented. The main achievements are described below:

- It has been demonstrated that graded SiGe photonics circuits epitaxially grown on Si substrate presents definitive advantage, as single waveguides can be used with low propagation losses in an unprecedent wavelength range, up to 11 wavelengths, for both TE and TM polarization [1]. A whole set of passive devices has then been demonstrated such as optical spectrometers based on classical Fourier-transform approach [2-3].

- The possibility to achieve broadband light sources in the mid-IR based on supercontinuum generation has then been investigated. On- chip two-octave supercontinuum generation ranging from 3 to 13 µm has been obtained [4], benefiting from the unique features of Ge-rich graded SiGe waveguides, which allow for large Kerr coefficient (n_2 up to 2 10^{-17} m^2/W), second-order dispersion tailoring and low propagation losses over a wide wavelength range.

- On-chip optoelectronics devices have then been developed: (i) optical modulators based on free-carrier plasma dispersion effect in graded SiGe waveguide embedding a Schottky diode have been demonstrated. The main challenges for high-speed operation have been tackled, allowing to demonstrate 1 GHz operation in an integrated device operating from 5 to 9 µm wavelength [5] ; (ii) a waveguide-integrated photodetector has then been demonstrated for the first time in a similar wavelength range [6]. A responsivity reaching up to 0.1 mA/W has been obtained at room temperature, which opens strong perspectives for the development of compact and efficient spectroscopic systems exploiting synchronous detection or for on-chip monitoring.

The perspectives of these works will be discussed in the conclusion, both in terms of performance improvements and new developments towards on chip frequency comb generation.

Acknowledgements

This work is supported by ANR Light-up Project (ANR-19-CE24-0002-01) and by the French RENATECH network.

References

[1] M. Montesinos-Ballester, et al Optics Express, 28 (9), 12771 (2020).
[2] Q. Liu,et al, Optics Letters, 43 (20), 5021-5024 (2018).
[3] M. Montesinos-Ballester, et al, Scientific Reports, 9, 14633 (2019)
[4] M. Montesinos-Ballester, et al ACS Photonics, 7, 12, 3423–3429 (2020)
[5] T.H.N. Nguyen et al, Advanced Photonics Research, 2200237 (2022)
[6] T.H.N. Nguyen et al, Optics Express, 30, (26), 47093 (2022).

DC Kerr effect for high speed modulation

Jonathan Peltier [1,2], Weiwei Zhang [3], Leopold Virot [2], Christian Lafforgue [1], Lucas Deniel [1], Delphine Marris-Morini [1], Guy Aubin [1], Farah Amar [1], Denh Tran [3], Xingzhao Yan [3], Callum G. Littlejohns [3], Carlos Alonso-Ramos [1], David J. Thomson [3], Graham Reed [3], Laurent Vivien [1]

[1] *University Paris-Saclay, CNRS, Centre for Nanoscience and Nanotechnology (C2N), Palaiseau, 91120, France*

[2] *University Grenoble Alpes, CEA, LETI, Grenoble, 38000, France*

[3] *Optoelectronics Research Centre, Zepler Institute for Photonics and Nanoelectronics, Faculty of Engineering and Physical Sciences, University of Southampton, Southampton SO17 1BJ, UK*

jonathan.peltier@c2n.upsaclay.fr

Abstract

This work demonstrate high-speed optical modulation based on the electric field-induced Pockels effect in silicon PIN junction waveguides. The relative contributions of both plasma dispersion and Kerr effects are quantified and we demonstrate dominant optical modulation from Kerr effect under an external DC electric field.

Result

The DC Kerr effect originates from the third-order nonlinear susceptibility tensor $\chi^{(3)}$ in presence of a static electric field F_{DC}. Its corresponding refractive index change when an RF field $F_{RF}\cos\Omega t$ is superimposed and applied to the PIN junction (Fig. 1(a)) is:

$$\Delta n(t) = \frac{3\chi^{(3)}}{2n_{si}}\left(F_{DC}^2 + \frac{1}{2}F_{RF}^2 + 2F_{DC}F_{RF}\cos\Omega t + \frac{1}{2}F_{RF}^2\cos 2\Omega t\right) \tag{1}$$

An unbalanced Mach-Zehnder Modulator (MZM) is used to characterize this effect (Fig. 1(b)). Measurements of the Ω and 2Ω components of the MZM transfer function are used to calculate the contribution of the DC Kerr effect to the modulation at Ω (Fig. 1(c)) showing that it is greater than the carrier modulation above 5 V and reaches more than a factor of 3 at 15 V. A good agreement with simulations is obtained.

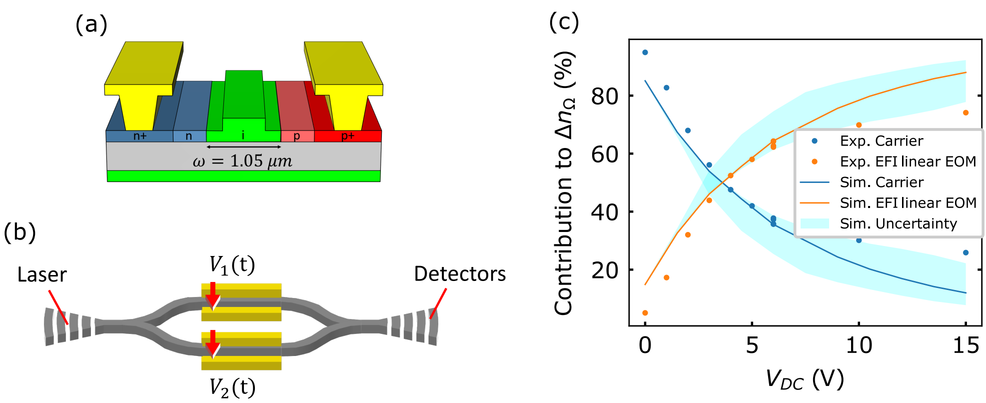

Fig. 1. (a) PIN junction depiction. (b) Schematic view of the experimental setup used to measure the EOM from the MZM (c) Relative contribution of index variation in the Ω component from EFI linear EOM and from carrier modulation versus the applied reverse DC bias voltage.

Design Strategy for Compact Mode-Division-Multiplexer for Multi-Channel Optical Interconnects

Jyoti Prasad Nath, Nikhil Dhingra, Geetika Jain Saxena and Enakshi K. Sharma *

Department of Electronic Science, University of Delhi South Campus, New Delhi – 110021, India
*** enakshi@south.du.ac.in**

We present the design considerations for a compact 3-channel mode division (de)multiplexer in silicon waveguides for on-chip optical interconnects consisting of two collocated asymmetric directional couplers to couple two independent signals into the TE_1 and TE_2 modes of 3-moded interconnect bus waveguide.

Introduction

The use of multicore processors requires a large electrical interconnect network which is bandwidth limited and has large ohmic losses. With integration of photonic circuits with electronic circuits, silicon-on-insulator (SOI) waveguides are emerging as a replacement to electrical interconnects.

Device Design and Optimization

To decrease the footprint, a multimode SOI bus waveguide can be used with each mode connecting an individual channel through (de)multiplexers. We have looked at a compact evanescent coupling based multiplexer with input waveguides arranged collaterally to form two collocated asymmetric directional couplers to couple two channels in one section as shown in Fig. 1a.The design requires a strategy validated here with a configuration of two input waveguides of width 484 nm and 302 nm phase matched to the TE_1 and TE_2 modes of a 220nm x 1.0 µm waveguide (Fig. 1b). First, the phase matched width has to be corrected for the presence of the other waveguides. Second, relatively large spacing between the waveguides ensures complete power transfer, but it results in (i) large coupling lengths (~95 µm) and (ii) very poor tolerance to small change in phase matched widths. Hence in a suitable design at the input and output end waveguides have a large spacing connected by an adiabatic transition to the primary coupling section with reduced spacing.

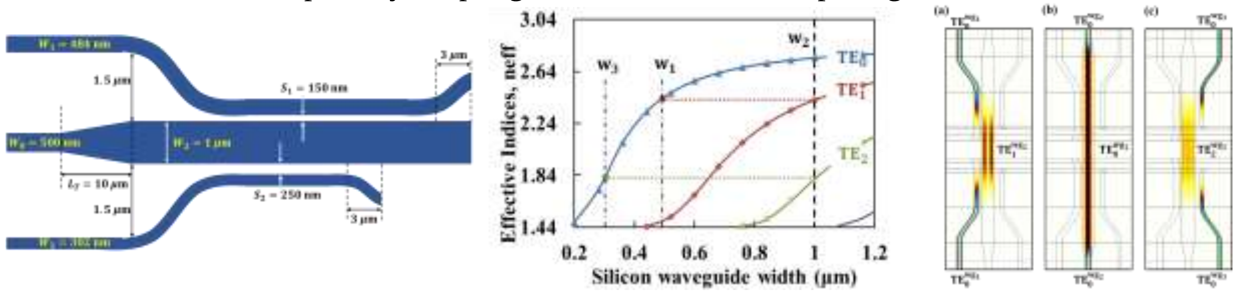

Fig.1. (a) (de)multiplexer for three mode multiplexing (b) Effective indices of TE modes versus the width of a 220 nm thick silicon waveguide at 1550 nm (c) propagation through the bus waveguide.

Conclusion

The propagation through the bus waveguide coupled/decoupled via mode of the respective input waveguides is shown in Figs. 1(c). The coupling length of the (de)multiplexer section is ~24 μm with an insertion loss of ~0.26 dB and crosstalk ~ -36 dB at the design wavelength of 1550 nm.

References

1. D.A.B. Miller, "Rationale and challenges for optical interconnects to electronic chips," Proc. IEEE, **88**(6), 728–749 (2000)
2. J.P. Nath, N. Dhingra, G. J. Saxena, and E. K. Sharma, "Compact Mode Division (de)Multiplexer Based on Collaterally Coupled SOI Waveguides," IEEE Photon. Technol. Lett., **32**(10), 595–598 (2020).

Lossless operation of high-contrast integrated optical waveguide gratings

Manfred Hammer *, Henna Farheen, Jens Förstner
Paderborn University, Theoretical Electrical Engineering, Paderborn, Germany
* *manfred.hammer@uni-paderborn.de*

Radiative losses in slab waveguide Bragg gratings of high index contrast can be fully suppressed, if these are excited by oblique semi-guided waves at large angles of incidence. For symmetric gratings, also polarization conversion is forbidden. Structures with parameters from silicon photonics serve as examples.

Oblique excitation of slab waveguide Bragg gratings

Wave propagation along finite waveguide gratings with high refractive index contrast and/or large corrugation depths tends to be accompanied by radiative losses, which are highly unwanted for applications such as optical signal-processing filters, sensors, or lasing reflectors. In that context, we explore the properties of gratings with simple rectangular corrugations and 1-D periodicity, as exemplified in the figure. The structures are excited by "semi-guided waves" that are strictly confined in the direction perpendicular to the guiding slab, that have in-plane the form of a plane wave, and that come in at the grating at an oblique angle. We show that, for a sufficiently high angle of incidence, radiation losses, originating either from the corrugated region or from the interfaces between the grating and the original slab, are (mathematically) strictly suppressed. In the band-structure analysis, the concept of a "light line" does not apply. Further, by virtue of symmetry arguments, polarization conversion is strictly prohibited.

Results for a series of fully- and partly-etched finite gratings are discussed, for SiO_2-embedded silicon slabs, specifically for TE excitation at an angle of 45°. The devices generate a reasonably flat-top wavelength response; apodization can lead to even more box-shaped spectra. TE transmittance and reflectance add up to one in all cases. Together with a narrow-band Fabry-Perot filter based on similar principles, these configurations exhibit reflection bands, or transmittance peaks, with widths that span three orders of magnitude.

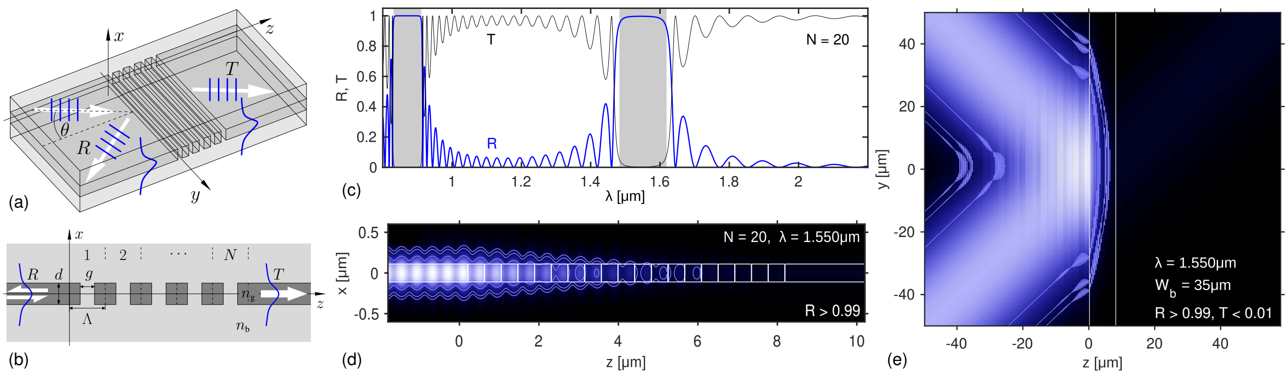

A symmetric slab waveguide grating, schematic (a), and cross-section view (b). Results for $N = 20$ periods, refractive indices $n_b = 1.45$, $n_g = 3.45$, thickness $d = 0.22\,\mu$m, period $\Lambda = 420$ nm, gap $g = 10$ nm, and incoming semi-guided TE waves at angle $\theta = 45°$: Reflectance R and transmittance T versus wavelength λ (c), energy density for plane wave excitation (d), and for excitation by a beam of width W_b (e), at $\lambda = 1.55\,\mu$m. (Figure adapted from Ref. [1])

References

[1] M. Hammer, H. Farheen, and J. Förstner. How to suppress radiative losses in high-contrast integrated optical gratings. Submitted for publication, 2023.

Modelling of a fully integrated graphene-based compact plasmon coupler

G. Renversez [1], A. Natarajan [1], G. Demésy [1],
[1] *Aix Marseille Univ, CNRS, Centrale Marseille, Institut Fresnel, Marseille, France*
gilles.renversez@univ-amu.fr

We describe the key elements that allow us to model rigorously a plasmon coupler located on the top of a planar waveguide. Two methods based on the finite element method are combined to reach this result: a modal solver and a scatterring method. They are used to design an efficient and compact coupler for the infrared.

Since the renewal of plasmonics in the last two decades, the generation and launching of surface plasmon polaritons (SPPs) has been a crucial problem both theoretically and experimentally [1, 2]. In fully integrated configurations based on optical waveguides useful to reach compactness and robustness for future photonic devices, one of the most efficient solutions that has been proposed is to use a metal grating to ensure the generation of surface plasmon polariton from the input beam. The grating allows to compensate the propagation constant mistmatch between the one of the mode that propagates in the input fully dielectric waveguide and the one of the plasmon mode that propagates in the output waveguide that is of plasmonic type due to the presence of an usually thin metal layer or a graphene one in our case. This concept of coupler to generate a SPP has already been proven experimentally in the mid-infrared near 8 µm with a gold grating [3].
In order to model the full device accurately and rigorously, the method we have recently developped to study discontinuities in waveguides within a full vector description given by Maxwell's equations is used [4]. It doesn't rely on any hypothesis regarding the sizes, the shapes or the permittivities of the discontinuities, without any approximation as long as only linear materials are considered. In the present study, the graphene grating will form the discontinuities. In this method, the incident mode of the input waveguide part of the photonic device is computed within the framework of the finite element method (FEM) in a modal approach. It is then injected as in incident field in the device containing the grating in a scattered field approach again within the FEM framework. The grating is followed by a continuous graphene sheet where the GP can propagate. All the physical quantities, either local or global, like the Poynting vector or the coupling efficiency can be computed accuretaly. The modeling of the graphene is done using a true 2D model in which the graphene as a 2D material is described by a 2D sheet with a complex conductivity described by the Kubo's model [4]. This accurate way to describe the graphene has at least two advantages compared to the more usual way where a finite thickness layer is artificially introduced to describe it. First, it avoids the studies of the dependency of the results as a function of the thickness artificial layer. Second, in 3D problems, it avoids to model a thick layer with 3D elements since only 2D elements are needed to mesh the graphene sheet. In 2D models like the one investigated here it avoids to model a thick layer with 2D elements. The FEM formalism we used to solve the 2D problem and its implementation using the open source softwares gmsh and getdp is also valid to tackle 3D problems.

References

[1] H. Ditlbacher, N. Galler, D. Koller, A. Hohenau, A. Leitner, F. Aussenegg, and J. Krenn, Opt. Express, vol. 16, no. 14, pp. 10 455–10 464, 2008.
[2] J.-P. Tetienne, A. Bousseksou, D. Costantini, Y. D. Wilde, and R. Colombelli, Opt. Express, vol. 19, no. 19, pp. 18155–18163, 2011.
[3] A. Babuty, A. Bousseksou, J.-P. Tetienne, I. M. Doyen, C. Sirtori, G. Beaudoin, I. Sagnes, Y. De Wilde, and R. Colombelli, Phys. Rev. Lett., vol. 104, p. 226806, 2010.
[4] G. Demésy and G. Renversez, J. Opt. Soc. Am. A, vol. 37, no. 6, pp. 1025–1033, 2020.
[5] J. Li, J. Tao, Z. H. Chen, and X. G. Huang, Opt. Express, vol. 24, no. 19, pp. 22 169–22 176, 2016.

Optimizing photonic devices: open-source implementation of auto-differentiable numerical methods

B. Vial [1],
[1] *Department of Mathematics, Imperial College London, London, United Kingdom*
b.vial@imperial.ac.uk

I will present the development of numerical methods for the resolution of Maxwell's equations implemented using open source libraries. All of them are endowed with automatic differentiation capabilities and typical inverse design examples using topology optimization will be presented.

Introduction

In the past two decades, gradient-based topology optimization (TO) has become a widely used tool in computational electromagnetism and has allowed the inverse design of a broad range of devices such as invisibility cloaks, metamaterials and metasurfaces to name a few.

Summary

I will detail the development of software libraries with automatic differentiation capabilities [1]: a Finite Element Method (FEM) based code for 2D scattering problems, an implementation of the Fourier Modal Method (FMM) for stacked bi-periodic structures and a Plane Wave Expansion Method (PWEM) to compute the eigenmodes of 2D photonic crystals. After describing the methods and the automatic differentiation and topology optimization tools, I will give examples of application for each: the design of supperscattering structures with the FEM, of a metasurface optimized to transmit maximally in a given diffraction order with the FMM and maximization of bandgap and dispersion engineering in dielectric photonic crytsals using the PWEM.

Results

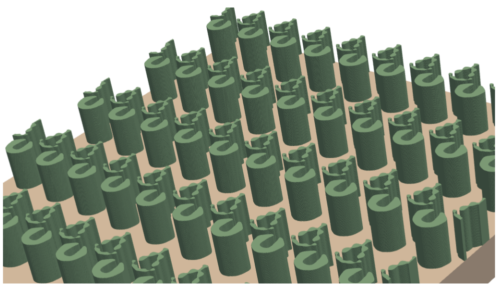

Fig. 1. Optimized metasurface blazed in the (1,0) transmitted order for both polarizations using the FMM.

Conclusion

The availability of open-source codes for solving Maxwell's equations is of paramout importance in the growing field of metamaterials and photonics. Our implementation of the three numerical methods commonly used in photonics is freely available as Python packages: https://gyptis.gitlab.io (FEM), https://nannos.gitlab.io (FMM) and https://protis.gitlab.io (PWEM).

References

[1] Benjamin Vial and Yang Hao. Open-Source Computational Photonics with Auto Differentiable Topology Optimization. *Mathematics*, 10(20):3912, January 2022.

Advancing wavefront shaping with resonant metasurface

Enzo Isnard [*,1,2], Sébastien Héron [2], Stéphane Lanteri [1], Mahmoud Elsawy [*,1]
[1] *Université Côte d'Azur, Inria, CNRS, LJAD, 06902 Sophia Antipolis Cedex, France*
[2] *THALES Research & Technology, 1 avenue Augustin Fresnel, 91120 Palaiseau, France*
enzo.isnard@thalesgroup.com *mahmoud.elsawy@inria.fr*

In metasurface design, the use of look-up tables based on a local periodicity approximation have been traditionally employed, but can result in sub-optimal designs due to lack of consideration of near-field coupling effects, which are particularly important for resonant systems. This paper explores the benefits of taking into account near-field coupling while optimizing non-local resonant metasurfaces to enhance their performance for wavefront shaping, including the state-of-the-art Huygens's metasurface.

Summary

Metasurfaces are two-dimensional planar structures constituted of sub-wavelength sized elements that can alter electromagnetic wave properties, including phase, amplitude, and polarization. Metasurfaces are generally locally approximated by periodic structures around each nano-element. This approximation allows the use of the look-up tables to design them, consisting in simulating the optical response of isolated nano-elements and placing them according to a phase profile given by the generalized Snell's law. In highly resonant structures the meta-atoms are not isolated and their response may depend on their neighbors, making the local periodicity approximation irrelevant. In our previous work, we exploited the benefits of global optimization coupled with full-wave solver to significantly improve the performances of metasurfaces [2, 3]. The present work considers resonant configurations including the state-of-the-art Huygens's metasurfaces where the apparition of collective resonances [4] makes the local periodicity assumption obsolete. We use Kriging-based Bayesian optimization as it is well suited for expansive black-box function and can be adapted to handle fabrication uncertainty [5] and multi-objective problems [3]. We illustrate our methodology in the case of a meta-deflector taken from ref. [1]. Figure 1 shows the deflection efficiency of both the optimized and the look-up table design, where simulations are performed using the software suite *DIOGENeS* [6] developed at *Inria Sophia Antipolis*. The drastic improvement of efficiency highlights the need for optimizing the whole period at once in the case of highly resonant structures.

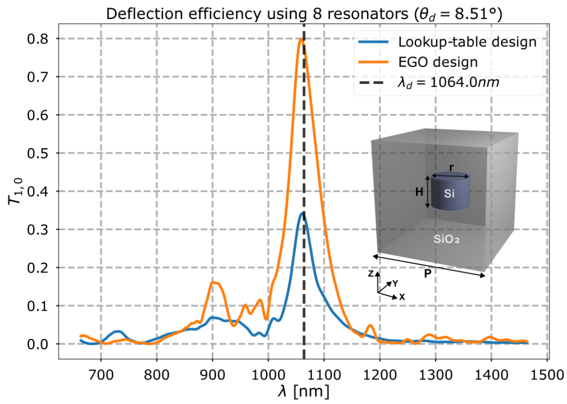

Fig. 1. Deflection efficiency of metagratings obtained with a look-up table and with global optimization. The inset indicates the schematic representation of the structure under consideration [1]

References

[1] A. Özdemir et al. Polarization independent high transmission large numerical aperture laser beam focusing and deflection by dielectric huygens' metasurfaces.
[2] M. M. Elsawy et al. Global optimization of metasurface designs using statistical learning methods.
[3] M. M. Elsawy et al. Multiobjective statistical learning optimization of rgb metalens.
[4] C. Gigli et al. Fundamental limitations of huygens' metasurfaces for optical beam shaping.
[5] M. M. Elsawy et al. Optimization of metasurfaces under geometrical uncertainty using statistical learning.
[6] *DIOGENeS : A Discontinuous-Galerkin based software suite for nano-optics.* https://diogenes.inria.fr/.

Inverse design of compact and broadband nanophotonic beamsplitters

Søren Engelberth Hansen[1,*], Guillermo Arregui[1], Rasmus Ellebæk Christiansen[2,3], Søren Stobbe[1,2]

[1] *Department of Electrical and Photonics Engineering, Technical University of Denmark, Denmark*
[2] *NanoPhoton - Center for Nanophotonics, Technical University of Denmark, Denmark*
[3] *Department of Mechanical Engineering, Technical University of Denmark, Denmark*

*senha@dtu.dk

We present the development of a compact broadband silicon photonics beamsplitter using inverse design by topology optimization. The proposed device achieves an excess loss of -0.11 dB at 1550 nm, a 1-dB bandwidth of 800 nm, and return losses below -15 dB for this range.

Photonic integrated circuits (PICs) have emerged as a crucial technology for modern communication systems and sensing applications, providing a high-speed, low-power, and compact platform for integrating multiple functionalities on a chip. To fully realize their potential, each circuit component must be carefully designed to provide high performance. In this work, we utilize the inverse design method known as density-based topology optimization [1,2] to obtain a compact and broadband nanophotonic beamsplitter. We define a design domain of 2 µm × 3 µm that can transfer light from one input waveguide into two output waveguides with symmetric 3-dB splitting. We optimize for maximum transmission and minimum reflection for three wavelengths, each separated by 100 nm, to provide broadband performance.

$$\min \Phi = 10 \sum_{i=1}^{3} s_i \log_{10}\left(\frac{T_{\text{port}-} + T_{\text{port}-3}}{1+R_{\text{port}-1}}\right) / \sum_{i=1}^{3} s_i,$$

Where s_i are scaling factors, T_i are the transmissions and R_i are the back-reflections. We solve the physics in a finite-element model and the optimization with a gradient-based solver with the final design respecting the fabrication restriction of electron-beam lithography. The obtained design for a beamsplitter with a 220 nm silicon device layer embedded in glass is shown in Fig. 1 with the electric-field profile (a) and the intensity (b) for the center wavelength as well as the broadband performance (c). Compared to other design approaches [3], we achieve a larger bandwidth within a very compact footprint, which is beneficial for compact multifunctional photonic integrated circuits.

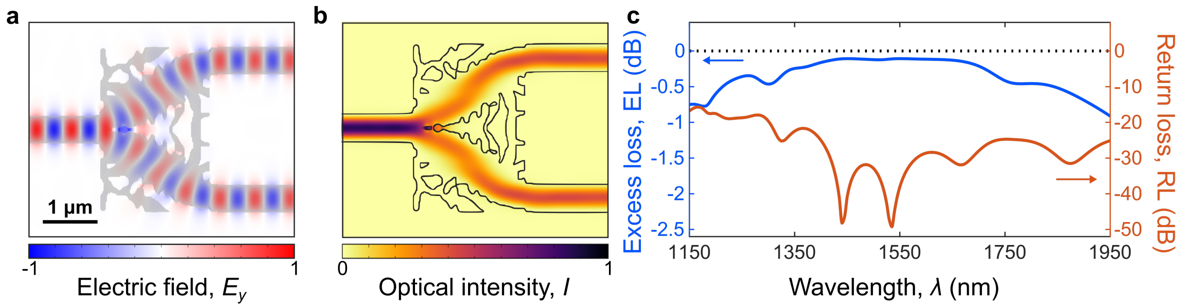

Fig. 1. A topology-optimized silicon beamsplitter with silica cladding. a. Transverse electric field (E_y). **b.** Optical intensity. **c.** Excess loss and return loss.

References

[1] R. Christiansen, O. Sigmund, *Inverse Design in Photonics by Topology Optimization: Tutorial.*, JOSA - B. 38, no. 2, p. 496-509, 2021.

[2] L. Frandsen, P. Borel, J. Jensen, O. Sigmund, *Topology Optimized Photonic Wire Splitters*, CLEO 2006 and QELS 2006, p. 1-2, 2006.

[3] D. González-Andrade, C. Lafforgue, E. Durán-Valdeiglesias, X. Le Roux, M. Berciano, E. Cassan, D. Marris-Morini, A. Velasco, P. Cheben, L. Vivien, C. Alonso-Ramos, *Polarization and Wavelength Agnostic Nanophotonic Beam Splitter*, Sci. Rep., vol. 9, no. 1, p. 3604, 2019.

Physically sound photonic structures designed using optimization

P. Bennet [1], D. Langevin [1], O. Teytaud [2], R. Smaali [1], E. Centeno [1], A. Moreau [1],
[1] *Université Clermont Auvergne, Clermont Auvergne INP, CNRS, Institut Pascal, F-63000 Clermont-Ferrand, France*
[2] *META AI Research Paris, France*
antoine.moreau@uca.fr

Numerical optimization of photonics structures, also called inverse design, is a technique which is particularly useful when no design rules are available that could guide the design of a complex photonic structure. However, optimization suffers from two problems (i) it is almost never possible to prove that a given solution is the true optimum and (ii) optimization algorithms tend to get stuck in local minima. We show here that it is possible, using a simple but rigorous methodology, to generate structures that are both efficient and physically understandable.

While many design rules or efficient algorithms are available for multilayered structures, studied for decades, when it comes to any other type of device, the versatility of these structures hinders from providing any guiding rule. A typical example would be photonic structures that can be put on top of a silicum substrate to be combined with electronic devices. From previous studies [1], it seems very likely that almost any function (like multiplexing) can be realized efficiently with miniturized structures. Most of the design techniques that are used rely on local optimization algorithms like BFGS which are very efficient at finding the nearest local optimum. In photonics however, because of the large number of resonance even simple structures can present, the number of local minima is usually very large. Since no criterium allows to assess whether a solution is optimal, we are left with wondering whether we can trust a solution provided by an algorithm.

We have tries to precise in which cases a solution can be trusted and in which it can not. Several criteria can be found that reinforce our trust in a solution : (i) when the same solution is found often by an optimization algorithm, which is generally not deterministic and has thus to be run many times [2] (ii) when the solution presents some kind of regularity (periodicity or slowly varying characteristics) (iii) when similar solutions can be found in nature [3] (a criterium which is hard to meet) and finally (iv) when the structure can be analyzed and understood a posteriori. When several of these criteria are met, a solution can eventually be deemed satisfying.

Applying such criteria to determine if optimizations can be stopped or other optimizations should be run allows to produce better solutions, that, often, can be considered satisfying. Showing that a solution can be analyzed and understood is work intensive, but truly reinforce the trust that can be placed in a it. We will present several of these solutions, in a large variety of cases. Such solutions allows, too, to determine which algorithms are efficient at finding such solutions more easily [4], wich is critical in this search for new structures in photonics.

References

[1] Molesky, S., Lin, Z., Piggott, A. Y., Jin, W., Vucković, J., and Rodriguez, A. W. *Inverse design in nanophotonics.* Nature Photonics, 12(11), 659-670 (2018)

[2] Centeno, E., Alvear-Cabezón, E., Smaali, R., Moreau, A., and Taliercio, T. *Inverse-designed terahertz modulators based on semiconductor multilayers.* Semiconductor Science and Technology, 36(8), 085014 (2021)

[3] Barry, M. A., Berthier, V., Wilts, B. D., Cambourieux, M. C., Bennet, P., Pollès, R., ... and Moreau, A. *Evolutionary algorithms converge towards evolved biological photonic structures.* Scientific reports, 10(1), 12024 (2020)

[4] Teytaud, O., Bennet, P., and Moreau, A. *Discrete global optimization algorithms for the inverse design of silicon photonics devices.* Photonics and Nanostructures-Fundamentals and Applications, 52, 101072 (2022)

Homogenization and optimization of plasmonic metasurfaces

N. Lebbe [1], K. Pham [2], A. Maurel [3],
[1] *LAPLACE, CNRS, INPT, UPS, Université de Toulouse, France*
[2] *IMSIA, CNRS, EDF, CEA, ENSTA Paris, Institut Polytechnique de Paris, France*
[3] *Institut Langevin, ESPCI Paris, Université PSL, Sorbonne Université, Université de Paris, CNRS, France*
nicolas.lebbe@laplace.univ-tlse.fr

The homogenization theory is used to replace non-periodic plasmonic metasurfaces with effective transition conditions involving dispersive and spatially variable susceptibilities. An efficient approach for the design of metasurfaces is proposed by combining FEM simulations of the homogenized model and adjoint calculations.

Homogenization of plasmonic metasurfaces with Generalized Sheet Transition Conditions

In the last decades, models reducing the geometric complexity of a metasurface into planar interfaces with effective transition conditions have been developed. These are known as Generalized Sheet Transition Conditions (GSTC) [1] which replace the continuity of $[\![\mathbf{E}]\!] \times \mathbf{n}$ and $[\![\mathbf{H}]\!] \times \mathbf{n}$ (where $[\![\cdot]\!]$ denotes the jump between two mediums and $\mathbf{n}$ the normal vector) with

$$[\![\mathbf{E}]\!] \times \mathbf{n} = i\omega\mu_0 \mathbf{M}_{\parallel} - \nabla_{\parallel} \times \mathbf{P}_{\perp} \quad \text{and} \quad [\![\mathbf{H}]\!] \times \mathbf{n} = -i\omega\varepsilon_0 \mathbf{P}_{\parallel} - \nabla_{\parallel} \times \mathbf{M}_{\perp}, \tag{1}$$

where $\mathbf{P}$ and $\mathbf{M}$ are adequate surface magnetization and polarization. For plasmonic metasurfaces, i.e., for particles (a.k.a. “meta-atoms”) with wavelength-dependent negative permittivities, we have shown in [2] that $\mathbf{M} = \mathbf{0}$ and $\mathbf{P} = \overline{\overline{\chi}}_{ee} \{\mathbf{E}\}$ where $\{\cdot\}$ is the mean field on the interface while $\overline{\overline{\chi}}_{ee}$ is obtained by solving electrostatic problems. Furthermore, the dispersion relation of the susceptibilities can be obtained through the solution of a single plasmonic eigenvalue problem.

Gradient-based optimization

Traditionally, the design of most metasurfaces is obtained by placing meta-atoms inducing a given phase shift calculated using a locally periodic approximation. Greater accuracy can be achieved using homogenization theory and eq. (1) through FEM simulations of the whole metasurface. Exploiting these fast simulations, the optimal distribution of the meta-atoms geometries is found by computing the gradient of given objective functions through adjoint calculations.

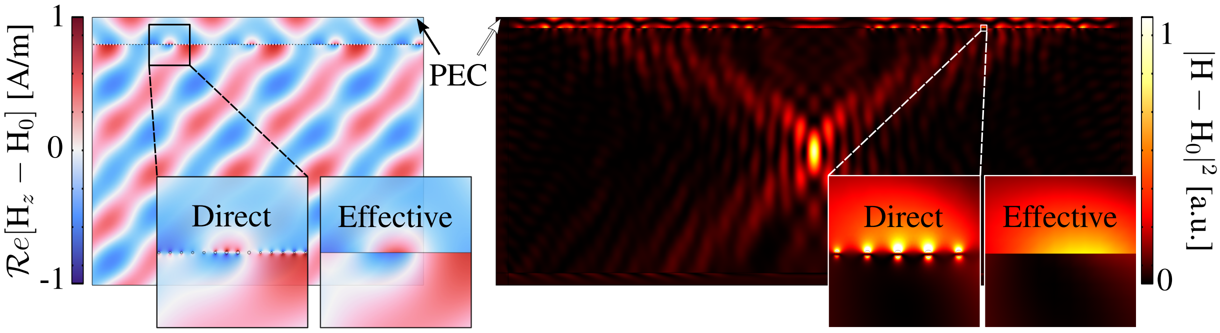

Fig. 1. Optimization of two reflective metasurfaces made of circular meta-atoms (ε = -1.05 - 0.001i) and zooms showing the adequation between direct and effective simulations; (left) meta-deflector (normal incident wave is reflected in the 4$^{\text{th}}$ order of diffraction) (right) meta-lens (the normal incident wave is reflected and focalized).

References

[1] N. Lebbe, K. Pham and A. Maurel *Stable GSTC formulation for Maxwell's equations,* IEEE Transactions on Antennas and Propagation, 2022.

[2] N. Lebbe, A. Maurel and K. Pham *Homogenized transition conditions for plasmonic metasurfaces,* accepted for publication in Physical Review B, 2023.

On the "Generalized" Snell-Descartes laws for metasurfaces

E. Rousseau D. Felbacq
Laboratoire Charles Coulomb – UMR5221, Université de Montpellier, Place Eugène Bataillon, France
emmanuel.rousseau@umontpellier.fr

We discuss the range of validity of the "generalized" Snell-Descartes laws for metasurfaces as introduced by the reference [1]. The discussion will follow two distinct roads. The first one introduces a phenomenological model that describes the physics of metasurfaces made by scattering elements. The second road questions the derivation of the "generalized" Snell-Descartes laws from the Fermat's principle.

Introduction

The laws of refraction and reflection are widely used to predict the intensity distribution of light by any imaging system. On the other hand, the "generalized" Snell-Descartes' laws for metasurfaces[1] are not or hardly used in practice to predict the distribution of the intensity of light in the presence of metasurfaces. Motivated by this observation, we revisit in details[2, 3] the proof of the "generalized" Snell-Descartes' laws. Based on two models, we show that none of these models reproduces the results given in [1].

Diffractive optics: A phenomenological model

The first model considers metasurfaces made by scattering nanoparticles, the case of most of the current experimental realizations. The physical mechanism at hand is based on diffraction. The calculations are carried in the Fraunhofer approximation. We show that this model reproduces all the experimental results but gives rise to "generalized" Snell-Descartes laws different from the published ones[1]. Particularly, we show that for metasurfaces with periodic pattern, the light distribution is given by the grating equation not by the "generalized" Snell-Descartes laws.

A model in geometrical optics

The derivation of the "generalized" Snell-Descartes laws given in[1] is based on the Fermat's principle. This principle does not describe diffraction processes. In order to verify whether the "generalized" Snell-Descartes laws can be derived from the Fermat's principle, we consider a model of metasurfaces consistent with the assumptions of geometrical optics. The metasurface is made by a layer with a position-dependent refractive index whose thickness is made arbitrary small. We solve[3] rigorously the eikonal equation describing the propagation of a light ray in such a medium. Again this model, based on Fermat's principle, does not reproduce the equations published in [1].

References

[1] Yu, N. and Genevet, P. and Kats, M. A. and Aieta, F. and Tetienne, J.-P. and Capasso, F. and Gaburro, Z. *Light Propagation with Phase Discontinuities: Generalized Laws of Reflection and Refraction* Science **334**:6054, 333–337 (2011)

[2] Rousseau, E. and Felbacq, D. *Concept of a generalized law of refraction : A phenomenological model.* ACS Photonics, **7**, 1649–1654 (2020)

[3] Rousseau, E. and Felbacq, D. *Detailed derivation of the generalized Snell-Descartes laws from Fermat's principle. To appear in* JOSA A (2023)

A General Theory on the Robustness of Bound States in the Continuum

Amgad Abdrabou[1], Lijun Yuan[2], Wangtao Lu[1], Ya Yan Lu[3]
[1]*School of Mathematical Sciences, Zhejiang University, Hangzhou, China*
[2]*School of Mathematics and Statistics, Chongqing Technology and Business University, Chongqing, China*
[3]*Department of Mathematics, City University of Hong Kong, Hong Kong, China*
mayylu@cityu.edu.hk

A bound state in the continuum (BIC) may or may not be destroyed by a small perturbation of the structure. It is shown that for each generic BIC, there is an integer n, so that the BIC persists under small structural perturbations with n (properly tuned) parameters. A general formula for n is proposed and validated.

Introduction

Photonic structures with high-Q resonances are essential for many practical applications, and they can be relatively easily realized by modifying ideal structures with a bound states in the continuum (BIC). When a structure with a BIC is perturbed, the BIC may be destroyed (becomes a resonant state) or may continue to exist with a slightly different frequency and a slightly different wavevector (if appropriate). Some BICs are robust against certain structural perturbations. To discuss the robustness of BICs, it is necessary to specify the perturbations precisely. If a BIC is not robust, it is usually but not always destroyed by a perturbation.

Theory

Our objective is to understand how a nonrobust BIC can continue to exist when the structure is perturbed. The idea is that if a perturbation contains a few parameters, then a BIC may exist in the perturbed structure, if the parameters are properly tuned. We show that for a generic BIC, there is a unique non-negative integer n, and it is the minimum number of parameters needed to preserve the BIC. It should be emphasized that the perturbation containing n parameters should satisfy some conditions related to periodicity and/or symmetry, but is still very general. If a BIC has $n = 0$, then it is robust with respect to the specific set of perturbations. If $n \geq 1$, then the BIC is nonrobust. A larger n implies that the BIC is more difficult to find.

More specifically, we start with a structure given by a dielectric function $\varepsilon_*(\mathbf{r})$, assume there is a BIC in that structure, introduce a set S of perturbations given by functions satisfying some periodicity and/or symmetry conditions, and consider a perturbed structure with $\varepsilon(\boldsymbol{r}) = \varepsilon_*(\boldsymbol{r}) + \delta F(\boldsymbol{r}) + \gamma_1 G_1(\boldsymbol{r}) + \ldots + \gamma_n G_n(\boldsymbol{r})$, where δ is a real small parameter, F, G_1, ..., G_n are functions in set S, γ_1, ..., γ_n are tunable parameters. We want to find the smallest integer n, and γ_1, ..., γ_n depending on δ, such that a BIC exists in the perturbed structure, for small but arbitrary δ, any $F \in S$, and generic G_1, ..., G_n in S. We propose the following general formula for n:

$$n = \sum_{k=1}^{K} I_k - M,$$

where K is the total number of linearly independent scattering solutions related to the open radiation channels, $I_k \in \{0, 1, 2\}$ is an index related to the k-th scattering solution, M is the degrees of freedom in the wavevector of the BIC. Each scattering solution gives rise to a scalar constraint which is in general complex. The integer I_k is the number of real constraints related to the k-th scattering solution, thus $I_k \leq 2$. Because of the symmetry, I_k may be reduced to 1 or 0. If the BIC exists in the perturbed structure, the wavevector may have also changed, giving rise to the term $-M$. Symmetry protected BICs typically have a zero wavevector (thus $M = 0$) and also $I_k = 0$ for all $1 \leq k \leq K$. The validity of the above formula has been verified for BICs in many different structures.

Leaky modes for waveguide response functions

Brian Stout [1], Isam Ben Soltane [1], Nicolas Bonod [2],
[1] *Aix Marseille Univ, CNRS, Centrale Marseille, Institut Fresnel, Marseille, France*
owtnm2023@fresnel.fr

We describe here the possibility of fully describing the response functions of waveguides using a combined 'leaky-normal' mode formalism. We review the famed 'normalisation' problem of the 'leaky' modes, but also address more recent developments like the determination of the 'regular' or 'non-resonant' contributions. We also adress the use of sum rules to compensate for the truncation of 'leaky' mode spectral expansions. This study is motivated by recent advances in the study of 'Quasi Normal Modes' in 3D scattering systems[1] and an S-matrix analysis of 1D slabs[2]. Concrete examples will be discussed in the case of 1D waveguides.

Introduction

'Leaky' modes play an important role in the theory of waveguides. A signature feature of the leaky modes is that their time-harmonic descriptions diverge at large distances from the waveguide. Although the mathematical origin of this divergence is well understood, it has nevertheless been a long standing impediment to using leaky modes as basis functions for quantitative descriptions of the full waveguide response functions (which would also require the inclusion of the 'ordinary' guided waves).

Summary

Recent progress in leaky mode analysis and normalization and S-matrix analysis, indicate that it is possible to fully describe the quantitative response of a waveguide via its S-matrix the relies on a spectral expansion of its ordinary and leaky modes.[1,2] Such formulations should facilitate the descriptions of broad-band and temporal response of a waveguide. We shall being by reviewing the procedures for correctly 'normalising' the spatially divergent leaky modes in different spatial dimensions. Achieving the correct normalisation of the modes, although crucial, is not the whole story, and we will also discuss methods for completing the 'regular' or 'non-resonant' contributions that must be added to the modal contributions of the response functions. This work concludes with a discussion of the sum rules that leaky-mode eigenstates must satisfy and how they can be used to detect 'missing' modes or to compensate for the effects of modes that are voluntarily excluded from the spectral expansion description.

References

[1] *Derivation of the Transient and Steady Optical States from the Poles of the S-Matrix,* Ben Soltane *et al*, Laser & Photonics Reviews, 2200141, (2022).
[2] *Spectral expansions of open and dispersive optical systems: Gaussian regularization and convergence* Stout *et al*, New Journal of Physics 23, 083004, 2021.

A description of MOSEM – Multiple-Order Singularity Expansion Method – and its interest for studying light scattering

I. Ben Soltane[1], R. Colom[2], B. Stout[1] and N. Bonod[1]

[1] *Aix Marseille Univ, CNRS, Centrale Marseille, Institut Fresnel, 13013 Marseille, France*
[2] *CNRS, CRHEA, Universite Cote d'Azur, 06560 Valbonne, France*

The behaviour of physical systems can often be described using the Linear and Time-Invariant System (LTIS) model, which is useful to derive the response of a system to an excitation [1,2]. LTIS are usually characterized by their transfer function in the harmonic domain, defined as the ratio of the complex amplitude of the output and input signals. In particular, the S-matrix used in the scattering operator formalism can be directly linked to LTIS by considering each of its component as a transfer function. It has long been known that transfer functions can be expressed in terms of their zeros or residues and their singularities. Two main approaches exist. (i) A local approximation as a ratio of polynomials [3] (ii) An expansion of the transfer function in terms of its singularities and their associated residues. This is known as the Singularity Expansion Method [4,5]. Both the common zero and pole factorization, and the singularity expansion are local expressions, and physical interpretations may prove difficult to obtain close to the edges of the frequency windows. We show that these limitations can be overcome, and that a general, non-local expansion of the transfer function in terms of its singularities and Laurent series coefficients can be rigorously derived under simple, non-restrictive hypothesis. We call this expression the multiple-order singularity expansion method (MOSEM) [6], and show that it can be constrained by considering physically realistic signals, causality, passivity and stability. The case of a simple dispersive Fabry-Perot cavity [7], a slab of gold, is explored, where we apply MOSEM to the component of the S-matrix corresponding to the reflection coefficient to show that the reflected field can be reconstructed over the real frequency axis in the harmonic domain, and in the temporal domain by obtaining an accurate expression of the Impulse Response Function (IRF).

REFERENCES

[1] D'Azzo J. Linear control system analysis and design. (1983)

[2] Oppenheim A V, Buck J, Daniel M, Willsky A S, Nawab S H and Singer A. Signals & Systems. Prentice Hall (1997)

[3] Sanathanan C and Koerner J. Transfer function synthesis as a ratio of two complex polynomials. IEEE Transactions on Automatic Control 8 56–58 (1963)

[4] Baum C E. On the singularity expansion method for the solution of electromagnetic interaction problems. Tech. rep. AIR FORCE WEAPONS LAB KIRTLAND AFB NM (1971)

[5] Baum C. The singularity expansion method: Background and developments. IEEE Antennas and Propagation Society Newsletter 28 14–23 (1986)

[6] Ben Soltane I, Colom R, Dierick F, Stout B and Bonod N. Multiple-Order Singularity Expansion Method. arXiv 2302.01988 (2023)

[7] Ben Soltane I, Colom R, Stout B and Bonod N. Derivation of the Transient and Steady Optical States from the Poles of the S-Matrix. Laser & Photonics Reviews 2200141 (2022)

Poster presentations

Modelling of light scattering in resonant multilayered stacks

Y. Toumi [1], F. Lemarchand [1], C. Favard [2], J. Lumeau [1], G. Demesy [1,**], A. Lereu [1,*]
[1] *Aix Marseille Univ, CNRS, Centrale Marseille, Institut Fresnel, Marseille, France*
[2] *Institut de Recherche en Infectiologie de Montpellier, CNRS, Univ of Montpellier France*
[*] *aude.lereu@fresnel.fr*
[**] *guillaume.demesy@fresnel.fr*

In this paper we estimate the scattering effect induced by surface roughness within a multilayer using Finite Element Method. The investigated multilayers are designed to support optical resonance under total internal reflection TIR to improve fluorescence microscopy sensitivity.

Introduction

The surface topography is an important parameter to determine the response of a surface to an excitation beam. Roughness is a type of surface texture linked to high spatial frequency deviations that can parasite the optical response of multilayer-based components by introducing scattering and diffraction phenomena. This is especially the case with the considered resonant components working at incident angle larger than the critical angle [1].

Methods

In order to numerically study optical scattering [2] , we need first to model a geometrically limited rough surface due to the limited available computing resources. To this end, we need to truncate our domain and assume the roughness to be periodic of period d. We can then model this rough surface by sampling the original surface. The number of points gives the scattering frequency, which should be of the same order as the wavelength. The height of each point should be low compared to the layer's thickness, since we are working in the domain of small deviations [3]. To accurately determine the range of heights, we measured the roughness of a microscope slide using a profilometer. Finally, we replicate the same roughness pattern within the different layers of the considered stack as illustrated in Figure 1(left). We model the response of the obtained diffraction grating using Finite Elements as described in [4].

Results

Using a large period d, a large number of transmitted and reflected diffraction orders are obtained. The diffraction efficiency and angle associated to each order is computed and can be represented as a discrete radiation pattern as shown in Figure 1 (right). We compared the discrete radiation pattern while increasing d, the period of the grating, and found that beyond a certain value of d, the diffraction diagram remains unchanged, leading to results that are independent of d. We will discuss practical cases based on specific resonant multilayerd stacks.

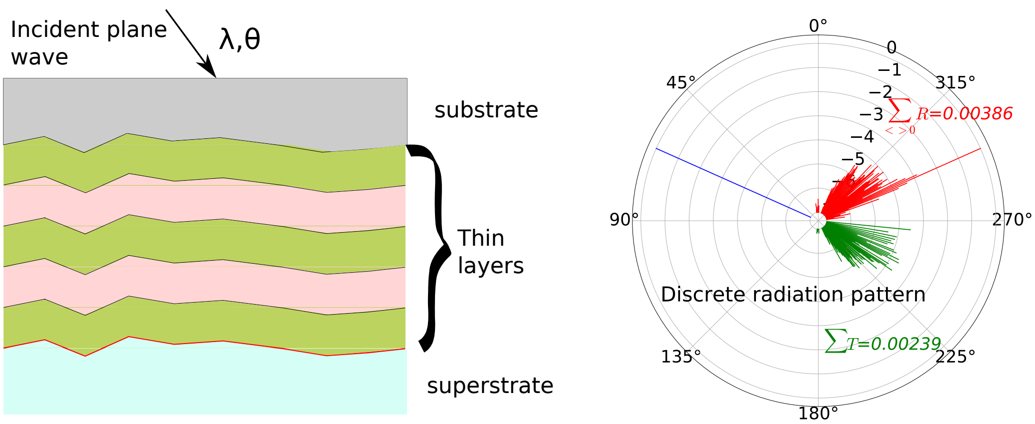

Fig. 1. (left): The geometry of the modeled structure (right):Angular distribution of the intensity

References

[1] Aude L Lereu, Myriam Zerrad, Césaire Ndiaye, Fabien Lemarchand, and Claude Amra. Scattering losses in multidielectric structures designed for giant optical field enhancement. *Applied optics*, 53(4):A412–A416, 2014.
[2] Claude Amra. Calculation and measurement of scattering for investigation of microroughness in optical coatings. *Journal of Optics*, 21(3):83, 1990.
[3] Dominique Meier. *Modélisation d'une interface rugueuse: études numériques et anaytiques*. PhD thesis, Le Havre, 2016.
[4] Guillaume Demésy, Frédéric Zolla, André Nicolet, Mireille Commandré, and Caroline Fossati. The finite element method as applied to the diffraction by an anisotropic grating. *Optics Express*, 15(26):18089–18102, 2007.

3D simulation of broad rejection band and ultra-narrow bandwidth hybrid Fabry-Pérot for guided optics

Jean Bittebierre

Aix Marseille Univ, CNRS, Centrale Méditerranée, Institut Fresnel, 13013 Marseille, France

Hybrid filters are **FPs** made up of a narrow band reflector, which is a Bragg grating with a low axial variation of refractive index Δn_L photo-written in a fibre or a waveguide, and a broadband reflector, which can be either a multilayer mirror **M** deposited at the end of the cleaved or polished photo-inscribed grating, or another **Bg** with a high axial index variation Δn_H (obtained by photo-refractivity or by ion implantation, and thus giving the possibility of a fibre technology as well as an integrated optics technology). This results in hybrid **FPs** that have a narrow Passband (PB = 100 pm to 10 fm) and a wide rejection (15 pm to 1 µm). The first essential condition for a hybrid **FP** to have 100% transmission at the top of its bandwidth is that it is balanced, i.e. that its reflectors have equal reflections. The second is to achieve phase matching between the periods of its reflectors. This phase matching can be achieved by adjusting the thickness of the layer adjacent to the **Bg** of the multilayer, or with a phase mask allowing a π phase jump between periods of **Bg** with $\neq \Delta n$. Whereas it is commercially available for identical **Bgs**, it requires innovation for **Bgs** with $\neq \Delta n$, which also have very $\neq$ lengths to be balanced. The 3D numerical simulations are done using Photon Design's Fimmwave/Fimmprop suite. They show that: 1) phase matching is fully controllable by the technologies mentioned, i.e. technically controllable errors will only cause a shift of the top of the PB without deforming it; 2) the hybrid **FPs** are only almost balanced due to the discrete character of the reflectors' reflection as a function of their period number; 3) the simple hybrid **FPs** are equivalent to an ideal **FP** with infinite planar mirrors, of equivalent length $L_{Eq} = x\, L_F$ where L_F is the length of the filter, and x is a coefficient only depending to the R reflexion common to both reflectors. Prototypes of single hybrid **FP** with a multilayer mirror have soon been achieved successfully.

Multiple hybrid **FPs** have a single PB only if they are constituted of an internal double hybrid **FP** surrounded by lateral **FPs** each constituted of 2 identical **Bgs** with the same Δn_L as this of the **Bgs** of the double hybrid **FP**. Simulations show that multiple hybrid **FPs** have several advantages soon since the double: 1) Bandwidth tails eliminated; Rejection highly increased; 3) sharper band edges with multiplicity. But in order that the filter has a single PB, the number of period of the **Bgs** of the balanced lateral **FPs** must be adjusted so that they have the same transmission spectrum as the single hybrid **FPs** of the inside double **FP**, and the multiplicity must stay to 3 or 4 at most. Multiple hybrid **FPs** are more difficult to achieve as they require even more innovation on the phase masks than single **FPs** with UV-written **Bg** broad band reflector, and because it is more difficult that the phase matching between the reflectors of all the single **FPs** contained centre their PB to the same wavelength. For too different centring the PBs of the single hybrid **FPs** do not overlap, and the transmission of the multiple hybrid **FP** is null. For hybrid **FPs** with multilayers, the number of independent phase matching can be reduced to 2 by achieving collective operations on fibre bundles, and by using symmetries for assembling.

Map of transmission coefficients for open bent waveguides with constant curvature

M. Sukhova [1], M. Paszkiewicz [2], W. Dörfler [1], C. Rockstuhl [2,3]
[1] *Institut für Angewandte und Numerische Mathematik (IANM), Karlsruher Institut für Technologie (KIT)*
[2] *Institut für Theoretische Festkörperphysik (TFP), Karlsruher Institut für Technologie (KIT)*
[3] *Institut für Nanotechnologie (INT), Karlsruher Institut für Technologie (KIT)*
mariia.sukhova@kit.edu

We are interested in studying light propagation in freeform open waveguides, i.e. photonic wire bonds. In this work, we present a calculation of transmission coefficients for an interface between two bent waveguide sections of various radii of curvature.

Summary

The transmission coefficients are applicable in the fast calculation of the transmission for the entire freeform waveguide, as done, for example, in [1] for the single-mode optical waveguide. Here we consider a photonic wire bond with two guided modes. At the junction of two sections of the waveguide with different radii of curvature, R_{L} (left) and R_{R} (right), a scattering problem arises, since one part of the guided modes is transmitted further and another part is decoupled. Our goal was to calculate the coefficients of such transmission t_{11}, t_{22}, t_{12} and t_{21} between modes. This was done for pairwise combinations of the radii of the curved segments in a range between 7 μm and 1000 μm. Since the considered waveguide segments have a constant curvature, we could find a semi-analytical solution following results in [2]. As a result, we obtained a pre-calculated database of transmission coefficients.

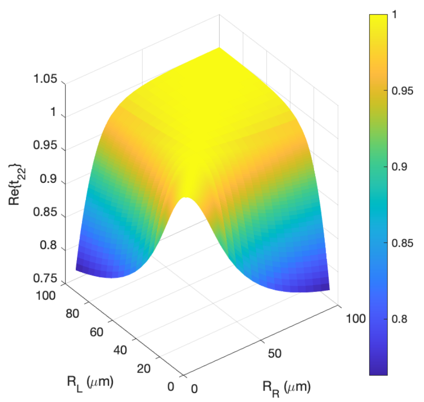

Fig. 1.: Transmission coefficients between curved waveguide segments with a radii of curvature R_{L} and R_{R}.

During the calculation of these values, we encountered some difficulties. The first one appears for the large radius $R = 1000$ μm. The computation of the semi-analytical solution is problematic since inside the waveguide's core Bessel's functions order and argument are large and almost equal in this case. Then, due to numerical cancellations for the Bessel's functions approximations, part of the solution inside the core is not stable and coefficients needed to couple the solution in the cladding and core are calculated incorrectly. To overcome this problem, we used the appropriate scaling for cylindrical functions and increased the precision to 30 decimal digits. Then we were able to calculate the transmission coefficients for the entire range of radii. The second difficulty was in choosing the integration interval since in order to calculate transmission coefficients, all solutions must be centered relative to the waveguide core, which requires the correct choice of the scalar product limits and cutting off solutions on the left side.

References

[1] F. Negredo, M. Blaicher, A. Nesic, P. Kraft, J. Ott, W. Dörfler, C. Koos, and C Rockstuhl. Fast and reliable method to estimate losses of single-mode waveguides with an arbitrary 2d trajectory. *JOSA A*, 35(6):1063–1073, 2018.

[2] K R Hiremath, M Hammer, R Stoffer, L Prkna, and J Čtyroký. Analytic approach to dielectric optical bent slab waveguides. *Opt. Quantum Electron.*, 37(1-3):37–61, January 2005.

Comparison of boundary integral equation methods for photonic crystal fibers with comsol Multiphysics simulation

M. Ayela [1], J-R. Poirier [1], H. Seat [2],
[1] *LAPLACE, Université de Toulouse, CNRS, INPT, UPS, Toulouse, France*
[2] *LAAS, Université de Toulouse, CNRS, INPT, UPS, Toulouse, France*
ayela@laplace.univ-tlse.fr

Boundary integral equation method is used to design photonics crystal fibers with many air holes and complicated geometries for innovative fiber-based refractometric sensor. Simulation output of the effective mode indices and the fields components

Introduction

Photonics crystal fibers (PCFs) have been extensively investigated because of their unique optical properties. PCFs with many air holes and complicated geometries can be difficult to analyse using conventional waveguide mode solvers such as the finite element method. In this work, we compare the simulation of PCFs by boundary integral equation methods with the Comsol Multiphysics software.

Results

Comparison of effective indices β/k_0 (step-index fibers).

Mode	Analytic solution	BIE solution
TM0m	1.43797885	1.43797885
TE0m	1.43798062	1.43796898

Comparison of effective indices β/k_0 (circular photonic crystal fibers).

Mode	Comsol Multiphysics	BIE solution
HEII	1.44539464-3.18614991E-8i	1.445395231561-3.19452295E-8i
HEII	1.44539457-3.18633520E-8i	1.445395231544-3.19443714E-8i

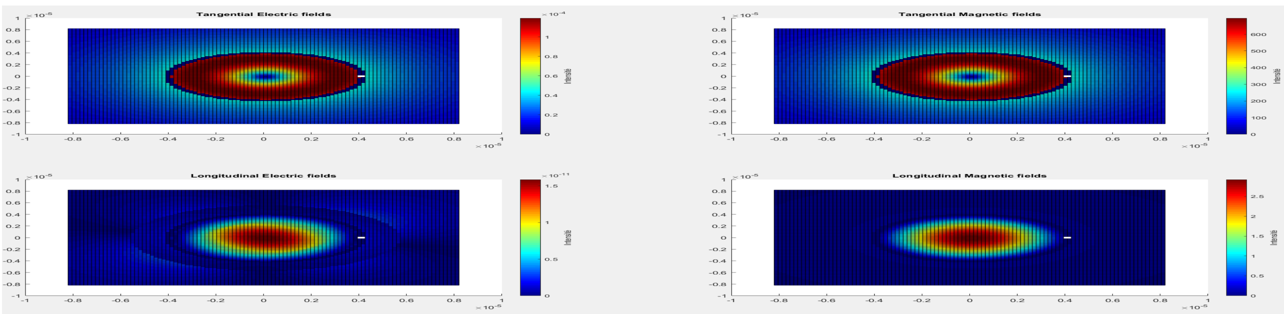

Fig. 1. Tangential and Longitudinal electric and magnetic fields.

Conclusion

Numerical results indicate that the new BIE method achieves exponential convergence and extremely high accuracy.

References

[1] W. Lu and Y. Lu *Efficient Boundary Integral Equation Method for Photonic Crystal Fibers,* Journal of Lightwave Technology, 2012.

Vector Mode Propagation in Graded Index Ring Core Fibers

Pratiksha Choudhary[1], Anurag Sharma[1,2]
[1]*Department of Physics, Indian Institute of Technology Delhi, New Delhi, 110016, India*
[2]*Optics & Photonics Centre, Indian Institute of Technology Delhi, New Delhi, 110016, India*[1]phz188425@iitd.ac.in; [2]asharma@iitd.ac.in

A finite differencefull vectorial propagation method is used to propagate vector modes through graded-index ring core fibers (GIRCF). Stability and accuracy of the method is also discussed.

Summary

Ring core fibers (RCF) are being examined for propagation of higher order modes and optical OAM modes for space-division multiplexing applications [1]. Graded-index ring core fibers (GIRCFs) offer advantage in terms of separation of vector modes and low propagation loss [2]. The vector mode analysis is important in understanding the wave propagation in these fibers. We show that our full vectorial non-paraxial method [3] can be easily used to analyze propagation through GIRCFs.

Results

We consider, as an example, propagation of HE_{21} mode through a graded index (parabolic, α=2) ring core fiber. The refractive index for ring core and cladding is n_{max}=1.474, n_{min}=1.444, and average radius and the width of ring structure are R=7μm and W=3μm,respectively and the wavelength used is 1μm.We have used 101×101 finite difference grid. The results are shown in the figure. More results will be presented at the Workshop.

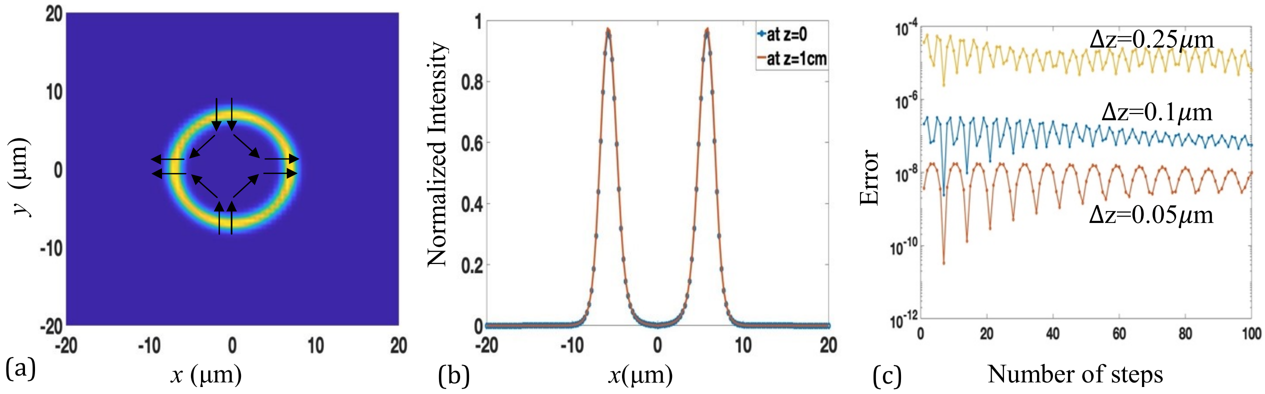

Fig: (a) Intensity profile of HE_{21} modewith direction of electric field indicatedby arrows, (b) the incident field intensity at z=0 and the field intensity after 1cm propagation at y=0 line are shownand (c) plots of error with propagation steps for differentΔz are shown.

Work partially supported by UGC fellowship to P. Choudhary & SERB J.C.Bose fellowship to A. Sharma.

References

[1] C. Brunet, B. Ung, P. A. Belanger, Y. Messaddeq, S. LaRochelle, and L. A. Rusch, "*Vector mode analysis of ring core fibers: Design tools for Spatial Division Multiplexing*," J. Light. Technol, vol. 32, issue 23, pp. 4046–4057, (2014).

[2] F. Feng, X.Guo, G. George S.D. Gordon, "*All-optical Mode-Group Division Multiplexing Over a Graded-Index Ring-Core Fiber with Single Radial Mode*,"Optical Fiber Communications Conference and Exhibition(OFC),Anaheim, CA, USA, pp. 1-3,(2016).

[3] P. Choudhary, A. Sharma, "*3-D Scalar and Vector Finite Difference based Modal and Propagation Methods*," Conference on Optics, Photonics & Quantum Optics (COPaQ),IIT Roorkee, November 10-13 (2022).

Design of nanostructured blazed gratings for spectro-imagers in space

Simon Ans [1,2], Guillaume Demésy [2], Frédéric Zamkotsian [1]
[1] *Aix Marseille Univ, CNRS, CNES, LAM (Laboratoire d'Astrophysique de Marseille), Marseille, France*
[2] *Aix Marseille Univ, CNRS, Centrale Marseille, Institut Fresnel, Marseille, France*
simon.ans@lam.fr

Spectro-imaging is one of the fundamental tools of astronomical observation, based on a state-of-the-art technology of optical instrumentation. We report on the mathematical modelling and the first developments of a meta-surface pattern that would enable an optimized diffraction efficiency on a wavelength broad band.

Context. For Earth and Universe observation purpose, a new generation of compact spectro-imagers is being developed [1]. A meta-surface blazed grating is therefore proposed in order to efficiently disperse the incident light on a wider range of wavelengths than a classic triangular blazed grating.

Mathematical model of a periodic structure. In the context of this project, an efficient light disperser refers to a blazed device that reflects most of the incident field on the -1 diffraction order. It leads to one particular outcome : the spatial space shift of the diffracted field should be controlled. Based on the results provided by [2] and using the Finite Element Method, a mathematical model is built and numerically implemented to design a meta-surface that controls the phase shift on reflection. It handles a given mono-dimensional grating under a conical incidence.

First design and results. The grating is a dielectric pattern (such as SiO_2, TiO_2, Nb_2O_5) structured on a reflective surface (silver, gold). It induces the spatial shift of a plane wave reflected on the -1 diffraction order in terms of relative refractive index (with pillar size ranging from 314nm to 17nm, see Fig. 1 a). It leads to the spectrum of diffraction efficiencies on Fig. 1 b and diffracted fields such as on Fig. 1 c for the wavelengths with the best reflection efficiencies. This structure is blazed indeed and the diffracted field is close to a plane wave reflected on the -1 diffraction order.

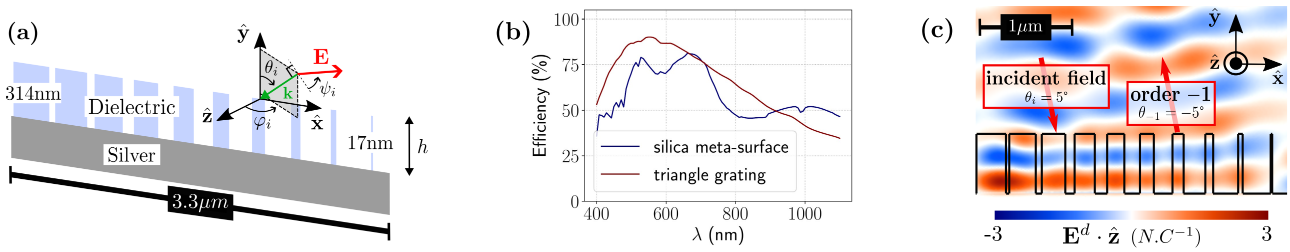

Fig. 1: **(a)** Period of a 2D dieletric meta-surface grating, section along the invariance axis. **(b)** Blazed efficiency spectrum on the -1 diffraction order obtained with this meta-surface on the 400-1100nm bandwidth, as compared to a classic triangular mirror grating, with silica ($h = 630$nm) as a dieletric and an incident field with $\theta_i = 5°$, $\varphi_i = -66°$ and $\psi_i = 90°$ (a transverse electric incidence 24° out of the Oxy plane). **(c)** The electric diffracted field for the same silica grating, at the wavelength $\lambda = 680$nm, projection on the Oxy plane.

The number of degrees of freedom for the grating performance optimization is significantly increased and the first results are promising. The next modelling step is thus based on the topology optimization of the grating and dual/multi blaze. The manufacturing of the first grating samples is under way.

References

[1] F. Zamkotsian, P. Lanzoni, N. Tchoubaklian et al. *BATMAN at TNG : Instrument integration and performance.* Proceedings of SPIE Astro, **10702**, 2018.

[2] G. Demésy, F. Zolla, A. Nicolet and B. Vial. *Gratings : Theory and Numeric Applications, Second Revisited Edition,* chap. 5. Aix Marseille Univ, CNRS, Centrale Marseille, Institut Fresnel UMR 7249, 2014.

Reliable automated classification of symmetry-induced degeneracy for numerically calculated guided modes

H. Lüder*, A. Uvarov, S. Mingaleev, I. Koltchanov, A. Richter
VPIphotonics GmbH, Carnotstr. 6, 10587 Berlin, Germany
*hannes.lueder@vpiphotonics.com

Waveguides with symmetries may support degenerate modes, which are difficult to identify numerically based on their effective indices. We show for representative waveguide geometries that an overlap integral-based criterion that takes into account the waveguide's symmetry group allows for reliable automated mode classification.

Optical waveguides with geometrical symmetries may support degenerate guided modes [1]. Analyzing such waveguides with numerical methods such as finite-difference-based mode solvers poses challenges: due to limitations in numerical accuracy or symmetry breaking through the mesh, degenerate and non-degenerate modes may have nearly identical eigenvalues, rendering them difficult to classify correctly. Furthermore, as degenerate modes span a multi-dimensional eigenspace associated with one eigenvalue, the mode solver may present any superposition as "the" modal field, which may differ from the expected TE/TM- or EH/HE-like mode field distributions.

Waveguides with C_n or $C_{n\mathrm{v}}$ symmetry support only non-degenerate and twofold degenerate modes [1]. The following criterion for classifying these modes is known [2]: a mode m is non-degenerate if for all symmetry operations S supported by the waveguide geometry the following condition holds:

$$|\langle m, S\, m\rangle| = 1. \tag{1}$$

Otherwise, it is degenerate. Here, $\langle \mu, \nu\rangle = \frac{1}{2}\iint \underline{\vec{E}}_\mu \times \underline{\vec{H}}_\nu^* \cdot \mathrm{d}\vec{S}$ denotes the classical inner product of guided modes. We use VPIdeviceDesigner's finite-difference mode solvers to calculate guided modes in symmetric waveguides commonly used in integrated photonics and fibre optics. We show that criterion (1) provides a numerically reliable way to identify degenerate modes. Once identified, we apply Gram–Schmidt orthonormalization to the degenerate modes to achieve reproducible mode profiles that enable reliable mode tracking in e.g. wavelength and geometry parameter sweeps.

The figure shows an exemplary hexagonal waveguide with $C_{6\mathrm{v}}$ symmetry. Because the rectangular mesh breaks the symmetry, all modes are numerically non-degenerate and the effective indices provide no sufficient means to classify them. However, criterion (1) clearly shows that modes (c) and (d) are degenerate, whereas (b) and (e) are not.

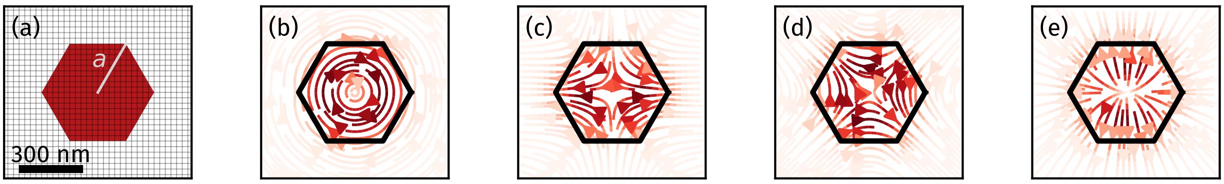

$a = 300\,\mathrm{nm}$, $n_{\mathrm{core}} = 2.0$ | $n_{\mathrm{eff}} = 1.7\mathbf{564}$, $\langle m, R_{60^\circ} m\rangle = 0.99$ | $n_{\mathrm{eff}} = 1.7\mathbf{203}$, $\langle m, R_{60^\circ} m\rangle = 0.41$ | $n_{\mathrm{eff}} = 1.71\mathbf{7}$, $\langle m, R_{60^\circ} m\rangle = 0.49$ | $n_{\mathrm{eff}} = 1.7\mathbf{027}$, $\langle m, R_{60^\circ} m\rangle = 0.91$

Figure. *(a) Hexagonal waveguide with rectangular mesh. (b)–(e) Electric field lines for non-degenerate and degenerate modes with their effective indices and the inner products with their 60°-rotated versions.*

References

[1] P. McIsaac. IEEE Trans. Microw. Theory Techn. 23 (5): 421–29, 1975. 10.1109/TMTT.1975.1128584
[2] M. J. Steel et al. Opt. Lett. 26 (8): 488–90, 2001. 10.1364/OL.26.000488

Second harmonic generation in cavity-resonator integrated grating couplers

A .-L. Fehrembach [1], E. Popov [1], H. Tortel [1], E. Hemsley [2],
A. Monmayrant [2], O. Gauthier-Lafaye [2], S. Calvez [2]
[1] *Aix Marseille Univ, CNRS, Centrale Marseille, Institut Fresnel, Marseille, France*
[2] *LAAS-CNRS, Université de Toulouse, CNRS, Toulouse, France*
mailto:anne-laure.fehrembach@fresnel.fr

Cavity resonator integrated grating filters (CRIGF) [1] are composed with a sub-wavelength coupling grating of a few tens of periods (GC), surrounded with two distributed Bragg reflectors (DBR), etched on a multilayer stack of lossless dielectric materials (see Fig. 1). Illuminated with an incident beam overlying the GC, CRIGF exhibit resonances characterized by a strong electromagnetic field. We are currently exploiting this property to enhance second harmonic generation (SHG) [2].

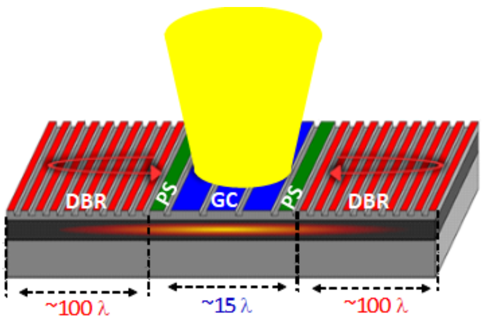

Fig. 1. Representation of a CRIGF.

In our first work [2], we reached numerically and experimentally a conversion efficiency $\eta = P_{2\omega}/[P_\omega]^2$ of the order of 8x10^{-6}W^{-1} (P_ω is the incident power and $P_{2\omega}$ is the power generated by SHG). This conversion efficiency is one order of magnitude higher than those achievable with infinite resonant gratings, but two orders of magnitude lower than those of the much longer ribbon guide components. In this presentation, we will show that the SHG conversion efficiency of the CRIGF can be improved by increasing the quality factor Q (ratio of the resonance wavelength to its spectral width) of the resonance at ω. We will describe two ways to achieve this: using a quasi-dark mode [3], or a GC with a bi-atom base pattern [4]. The high quality factors achieved (above 10^5) highlight the existence of a critical coupling regime [5,6], for which the SHG conversion rate is maximal. We demonstrate numerically conversion efficiencies of the order of a few tenths.

Acknowledgements: this work was supported by the AID (ANR-ASTRID RESON project).

References

[1] K. Kintaka et al. *Cavity-resonator-integrated grating input/output coupler for high-efficiency vertical coupling with a small aperture* Opt. Lett. 35, pp. 1989-1991, 2010.
[2] F. Renaud et al. *Second-harmonic-generation enhancement in cavity resonator integrated grating filters* Opt. Lett. 44, pp. 5198-5201, 2019.
[3] Fehrembach et al. *Dark mode-in-the-box for enhanced second-harmonic generation in corrugated waveguides* Opt. Expr. 29 (25), pp 40981 (2021).
[4] Fehrembach et al. *Cavity-resonator integrated bi-atom grating coupler for enhanced second-harmonic generation* Opt. Expr. 30 (21), pp 38789 (2022).
[5] A. Yariv *Universal relations for coupling of optical power between microresonators and dielectric waveguides* Electron. Lett. 36 (4), pp321-322 (2000).
[6] Popov et al. *Extreme enhancement of the quality (Q)-factor and mode field intensity in cavity-resonator gratings* Opt. Expr. 30 (14), pp25390 (2022).